Master stability functions reveal diffusion-driven pattern formation in networks

Andreas Brechtel,[1] Philipp Gramlich,[1] Daniel Ritterskamp,[2] Barbara Drossel,[1] and Thilo Gross[2]
[1]*Institute of Condensed Matter Physics, Technische Universität Darmstadt, 64289 Darmstadt, Germany*
[2]*Department of Engineering Mathematics, Merchant Venturers School of Engineering, University of Bristol, Woodland Road, Bristol BS8 1UB, United Kingdom*

(Received 4 April 2017; revised manuscript received 8 October 2017; published 19 March 2018)

We study diffusion-driven pattern formation in networks of networks, a class of multilayer systems, where different layers have the same topology, but different internal dynamics. Agents are assumed to disperse within a layer by undergoing random walks, while they can be created or destroyed by reactions between or within a layer. We show that the stability of homogeneous steady states can be analyzed with a master stability function approach that reveals a deep analogy between pattern formation in networks and pattern formation in continuous space. For illustration, we consider a generalized model of ecological meta-food webs. This fairly complex model describes the dispersal of many different species across a region consisting of a network of individual habitats while subject to realistic, nonlinear predator-prey interactions. In this example, the method reveals the intricate dependence of the dynamics on the spatial structure. The ability of the proposed approach to deal with this fairly complex system highlights it as a promising tool for ecology and other applications.

DOI: 10.1103/PhysRevE.97.032307

I. INTRODUCTION

The study of complex networks has revealed many new interconnections between fields within the realm of complex systems, such as nonlinear dynamics and chaos, data analysis, cellular automata, graph theory, phase transitions, and pattern formation. For these areas, networks provide an overarching mathematical framework that is conducive to a unification of complex system theory [1]. This paper makes a contribution toward this goal by analyzing a general network formulation of diffusion-driven pattern formation. Our analysis points to an analogy between diffusive instabilities in continuous space and diffusive instabilities in networks. In both types of systems, these instabilities can be described by structurally identical equations. Analyzing pattern formation in complex networks is therefore not more difficult than analyzing pattern formation in continuous space, but tends to produce richer behavior.

Diffusion-driven instabilities in reaction-diffusion systems in continuous space were first discovered by Turing [2] and later independently by Gierer and Meinhard [3]. For such systems it is well known that diffusion of one type of agent without reactions leads to a homogeneous distribution. Such homogeneous states also exist in reaction-diffusion systems where multiple species interact with themselves or each other while undergoing the diffusion process [2]. In the continuous space reaction-diffusion system, these homogeneous states are stationary but not necessarily stable to perturbations. When critical parameter values are crossed, their stability is lost in bifurcations, which mark the onset of pattern formation. These can be either Turing bifurcations, leading to stationary patterns, or wave instabilities, leading to traveling wave patterns [2].

Nakao and Mikhailov [4] and later Fernandes and de Aguiar [5] investigated examples of pattern forming instabilities on networks. In their systems agents of different species "diffused" by undergoing a random walk on a network. Reactions between the agents then led to a Turing-type diffusion-driven instability and subsequent pattern formation.

In this paper, we take the idea and formalism of Nakao and Mikhailov further and formulate an analytical theory of diffusion-driven instabilities in networks. We analyze systems that comprise a large number of different species subject to nonlinear interactions. There are thus two networks, the underlying geographical network on which the species diffuse, and a network of interactions between species. While the species differ in the nature of their interactions, they diffuse on the same geographical network, albeit potentially at different rates. We show that such network-on-network systems follow the same laws as the continuous space reaction-diffusion system, but can exhibit more complex behavior.

Our derivation uses an approach that is formally equivalent to the master stability function technique that is widely used to study the stability of limit cycles in coupled oscillator systems [6,7]. This work thus touches on two very active areas, the study of synchronization[7,8] and multilayer networks [9–12], which is the subject of several recent reviews [13–18]. These two areas already have a wide interface due to many very recent papers, which studied synchronization on multilayer network [15,19–25].

The present work differs from the past papers in a number ways. Although some previous works investigated pattern formation in multilayer networks [19,21], these papers focused on interlayer effects in networks where the layers have different topologies. By contrast, we consider intralayer effects, in a more restricted class of systems, which allows deeper analysis and thus reveals the analogy to the continuous case.

Previously, the master stability function approach was widely used for the study of synchronization in multiplex networks [15,20,22–25], but again the focus of these works was on interlayer effects. Another difference to previous work is that we focus fundamentally on stationary states. Master

stability function approaches have so far only been used in synchronization where they are applied to limit cycles. Although a synchronized state in a system of phase oscillators is mathematically a steady state, one still thinks of it as a state in a system of coupled identical oscillators. Here, we present a derivation of the master stability function in the context of pattern formation and show that the application of the master stability function approaches to stationary states has great, presently untapped potential to lead to progress in applications.

We illustrate the potential of the approach by analyzing a complex ecological meta-food-web model. If one were to reduce ecology to a single question, this question would probably focus on the origin and maintenance of biodiversity. In the words of Hutchinson, "Why are there so many kinds of animals?" [26]. Much current research in ecology is aimed at understanding how diversity is maintained and specifically how different species manage to coexist [27]. Over the past three years, two major approaches to this question have been converging. One of these is the study of ecological food webs, the networks of who-eats-who in ecology. Here, a major question is what properties stabilize the food web [27–29]. Theoretical insights in this area are still largely gained from simulations [27]. However, the timescale separation between species on higher and lower trophic levels is a major obstacle that strongly limits the size of systems that can be simulated.

The second avenue of investigation asks how spatial distribution affects the persistence of species. Early models considered only a single species in space, a so-called metapopulation [30–32]. These models were subsequently extended to metacommunities, systems of competing similar species, e.g., different grasses in grassland plots. Only very recently predator-prey interactions have been introduced to this line of ecological modeling [33–38]. While the importance of such multilayer interactions for ecology has recently been emphasized [39,40], the considerable complexity of the resulting models has limited investigations to either a small number of species or a small number of spatial nodes.

Using the approach proposed here, we are able to study complex meta-food webs, which we illustrate in a 30-species example system on a spatial network of arbitrary size. For this purpose, we extend the so-called generalized food web model [28,36,41], to incorporate the dispersal of individuals across large networks of habitats or patches. The ecological model describes predator-prey interactions in continuous time. It uses biologically realistic nonlinear interactions between species, and realistic scaling of dynamical time scales and diffusion rates with species body mass. For each such food web the proposed method yields a master stability function that reveals which spectral constraint the underlying geographical network must obey in order for the homogeneous steady state to be stable, and at what threshold parameter values pattern forming instabilities occur. These results remain valid for spatial networks of any size and provide the researcher with a principled approach to discussing what network features benefit stability and what hinders it.

The paper starts by revisiting diffusion on networks and comparing it to diffusion in continuous space in Sec. II. We then revisit diffusion-driven instabilities in continuous space in Sec. III before deriving the master stability function approach for diffusion-driven instabilities on networks in Sec. IV. We propose the ecological model in Sec. V and present results from its analysis in Sec. VI. Finally, we conclude with a discussion of the potential of the proposed approach for work in ecology and beyond in Sec. VII.

II. DIFFUSION ON NETWORKS

Let us recapitulate some well-known properties of diffusion in continuous space that carry over to a properly defined diffusion process on networks:

(i) Let $X(x,t)$ be the concentration of agents or particles as a function of space and time. Then, given some initial configuration, the time evolution is given by

$$\dot{X} = c\,\triangle X, \tag{1}$$

where c is a diffusion constant and $\triangle$ is the Laplace operator.

(ii) This equation is solved by

$$X(x,t) = \sum_n a_n \mathrm{e}^{c\kappa_n t}\boldsymbol{v_n}, \tag{2}$$

where κ_n and $\boldsymbol{v_n}$ are the eigenvalues and eigenfunctions of the Laplace operator on the spatial domain under consideration, and a_n are expansion coefficients determined by the initial state. For instance, on a rectangular domain the eigenfunctions are trigonometric functions, and on a circular domain they are Bessel functions. In both cases, the eigenvalues κ_n are wave numbers.

(iii) On a connected domain, the Laplace operator is a negative semidefinite operator with a single zero eigenvalue, and the corresponding eigenfunction is constant in space, such that

$$\lim_{t\to\infty} X(x,t) = \text{const.} \tag{3}$$

Diffusion in networks has been studied for a long time [1] and different types of diffusion processes on networks have been proposed. However, perhaps the most intuitive process is the following:

Consider a network of N nodes described by an adjacency matrix $\mathbf{A}$ such that $A_{ij} = 1$ if nodes i and j are connected and $A_{ij} = 0$ otherwise. On this network let $X_i(t)$ be the number of agents in node i. Agents undergo a random walk in continuous time, meaning that an agent has a constant probability density (per time) to transverse each link that is incident to its current node. Note that this means that agents leave nodes of higher degree more quickly, which is intuitive for instance if the agents are molecules diffusing between cavities in microfluidics and is also consistent with behavior observed in animals [42]. In situations where coupling strengths, i.e., link transversal probabilities, differ between or within networks, a weighted form of the adjacency matrix can be used where the nonzero elements A_{ij} can be different from 1. Such situations arise for instance when diffusion through links is distance dependent.

In the limit of large agent number, the time evolution of the system can be written as

$$\dot{\boldsymbol{X}} = -c\mathbf{L}\boldsymbol{X}, \tag{4}$$

where $\boldsymbol{X} = (X_1, \ldots, X_N)^{\mathrm{T}}$ and c is a coupling constant and $\mathbf{L}$ is the Laplace matrix [1]. The Laplace matrix is constructed by setting $L_{ii} = \sum_j A_{ij}$ and subtracting $\mathbf{A}$. For nonweighted networks where $A_{ij} \in \{0,1\}$, the diagonal elements of the

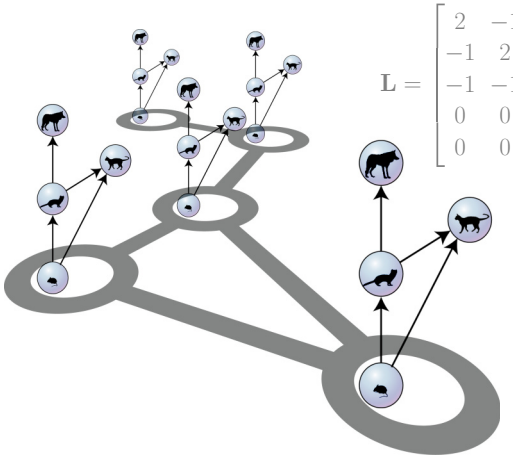

$$\mathbf{L} = \begin{bmatrix} 2 & -1 & -1 & 0 & 0 \\ -1 & 2 & -1 & 0 & 0 \\ -1 & -1 & 3 & -1 & 0 \\ 0 & 0 & -1 & 2 & -1 \\ 0 & 0 & 0 & -1 & 1 \end{bmatrix} \quad \mathbf{P} = \begin{bmatrix} P_{11} & P_{12} & P_{13} & 0 \\ P_{21} & P_{22} & P_{23} & P_{24} \\ P_{31} & P_{32} & P_{33} & 0 \\ 0 & P_{42} & 0 & P_{44} \end{bmatrix} \quad \mathbf{C} = \begin{bmatrix} C_{11} & 0 & 0 & 0 \\ 0 & C_{22} & 0 & 0 \\ 0 & 0 & C_{33} & 0 \\ 0 & 0 & 0 & C_{44} \end{bmatrix}$$

$$\mathbf{J} = \begin{bmatrix} \mathbf{P}-2\mathbf{C} & \mathbf{C} & \mathbf{C} & 0 & 0 \\ \mathbf{C} & \mathbf{P}-2\mathbf{C} & \mathbf{C} & 0 & 0 \\ \mathbf{C} & \mathbf{C} & \mathbf{P}-3\mathbf{C} & \mathbf{C} & 0 \\ 0 & 0 & \mathbf{C} & \mathbf{P}-2\mathbf{C} & \mathbf{C} \\ 0 & 0 & 0 & \mathbf{C} & \mathbf{P}-\mathbf{C} \end{bmatrix}$$

FIG. 1. Example meta-food web with four species (blue bubbles and black arrows) on five habitats or patches (gray lines and circles). The stability of the system is described by the 20×20 Jacobian matrix $\mathbf{J}$, which can be written as 5×5 matrix of 4×4 blocks. The blocks contain the intrapatch Jacobian matrix $\mathbf{P}$, describing the dynamics within one patch, and the coupling matrix $\mathbf{C}$, describing the dependence of migration rates on the population sizes, which is given here for a simple diffusion process. While the intrapatch Jacobian only appears on the diagonal of $\mathbf{J}$, the coupling blocks $\mathbf{C}$ occur in a pattern given by the Laplacian matrix $\mathbf{L}$ that encodes the structure of the patch network and is shown here for a coupling strength of 1.

Laplace matrix are identical to the degrees of the nodes (cf. Fig. 1 for illustration of the Laplacian). The Laplace matrix is aptly named as it can be interpreted as finite difference approximation to $-\triangle$ on a network [43].

Note that Eq. (4) is analogous to Eq. (1), except for an additional minus sign, which appears for historical reasons, as defining the Laplacian as a positive definite operator was thought to be advantageous in its original application.

By decomposing $\boldsymbol{X}$ into eigenvectors of $\mathbf{L}$ we find the solution

$$\boldsymbol{X}(t) = \sum_n a_n \mathrm{e}^{-c\kappa_n t} \boldsymbol{v_n}, \tag{5}$$

where a_n are again expansion coefficients determined by the initial state and κ_n and $\boldsymbol{v_n}$ are the eigenvalues and eigenvectors of $\mathbf{L}$. Note that Eq. (5) is the network analog of Eq. (2), except for the minus sign in the exponent.

For the Laplacian matrix, the row sum $\sum_j L_{ij}$ is zero in every row. Therefore, there is always an eigenvalue $\kappa_1 = 0$, and the corresponding eigenvector is $\boldsymbol{v_1} = (1,1,\ldots,1)$ [43–45]. For connected networks, this is the only zero eigenvalue of the Laplacian. Hence, for $t \to \infty$ all terms of the Laplacian vanish except the $n = 1$ term, and we are left with

$$\boldsymbol{X}(t \to \infty) = a_1 \boldsymbol{v_1}, \tag{6}$$

where a_1 ensures the correct normalization. This equation is the network analog of Eq. (3), as it implies that in the long run the system approaches a state where the concentration of agents is identical in each node.

In this section we have revisited a well-known line of reasoning showing that a simple diffusion process on networks behaves analogously to a diffusion process in continuous space. In particular, the Laplacian matrix of network science is the analog of the Laplacian operator in continuous space and the system can be solved by a decomposition into the eigenmodes of this operator. In both cases, this reveals that (on connected domains) only one eigenmode survives in the long-term dynamics, which is constant in space. Thus, the diffusion process approaches a state where the agents are uniformly distributed.

III. DIFFUSION-DRIVEN INSTABILITIES IN CONTINUOUS SPACE

Let us now consider the case where multiple species $X_1, \ldots, X_M$ of agents diffuse over a network while undergoing reactions.

In continuous space, this is well studied [46] and the following is known:

(i) The dynamics of a general reaction-diffusion system is given by equations of the form

$$\dot{\boldsymbol{X}} = f(\boldsymbol{X}) + c \triangle \boldsymbol{X}, \tag{7}$$

where $\boldsymbol{X} = (X_1(x), \ldots, X_M(x))$ is a vector of functions describing the distribution of the respective species in space, f is a vector-valued function describing the local reactions, and c is again a coupling constant.

(ii) If the corresponding nonspatial system

$$\dot{\boldsymbol{X}} = f(\boldsymbol{X}) \tag{8}$$

has a stationary state $\boldsymbol{X}^*$, then in the spatial system there is a corresponding homogeneous state in $\boldsymbol{X}^*(x)$, where the concentrations of agents are constant in space.

(iii) The stability of the homogeneous steady states can be analyzed by linearizing the dynamics around the steady state by setting $\boldsymbol{X} = \boldsymbol{X}^* + \delta$. This gives the equation

$$\dot{\delta} = \mathbf{J}\delta, \tag{9}$$

where $\mathbf{J}$ is the Jacobian matrix. The Jacobian matrix is a square matrix, whose linear dimension is the number of species M. We can compute it as

$$J_{ab} = \frac{\partial}{\partial X_b} \dot{X}_a \bigg|_* = \frac{\partial}{\partial X_b} [f_a(\boldsymbol{X}) + c \triangle X_a] \bigg|_* . \tag{10}$$

	Continuous Space	**Network**
Laplacian Operator	Laplace Operator $\triangle$	Laplace Matrix -$\mathbf{L}$
Eigenmodes	$\triangle v_n = \kappa_n v_n$	$\mathbf{L}\boldsymbol{v_n} = \kappa_n \boldsymbol{v_n}$
Reaction diffusion system	$\dot{\boldsymbol{X}} = f(\boldsymbol{X}) + \mathbf{C}\triangle\boldsymbol{X}$	$\dot{\boldsymbol{X}}_i = f(\boldsymbol{X}_i) - L_{ij}\mathbf{C}\boldsymbol{X}_j$
Diffusive Instability	$\mathrm{Re}(\mathrm{Ev}(\mathbf{P} + \kappa_n\mathbf{C})) > 0$	$\mathrm{Re}(\mathrm{Ev}(\mathbf{P} - \kappa_n\mathbf{C})) > 0$

FIG. 2. Analogy between diffusion in continuous space and in networks. To emphasize the similarity, we have written the network reaction-diffusion system [Eq. (12)] in matrix form and also allowed a coupling matrix $\mathbf{C}$ in the instability condition for the continuous space systems. While our derivation considered the simpler case where $\mathbf{C}$ is proportional to the identity matrix, such matrices appear in the case of cross diffusion where diffusion of one species depends on the concentration of other species [46]. While the concentrations $\boldsymbol{X}$ are position dependent in continuous space, the state of the system on a network is captured by a discrete set of variables $\boldsymbol{X}_i$, with i being the node index. See text for detailed derivations.

To avoid the spatial derivative, we can again decompose the $\boldsymbol{X}$ into eigenfunctions $\boldsymbol{v_n}$ of the Laplace operator which yields a Jacobian matrix for every eigenmode n,

$$J_{ab}^{(n)} = \left(\frac{\partial}{\partial X_b} f_a(\boldsymbol{X})\right)_* + c\kappa_n\delta_{ab} = P_{ab} + c\kappa_n\delta_{ab}, \qquad (11)$$

where κ_n is the eigenvalue corresponding to $\boldsymbol{v_n}$, δ_{ab} is the Kronecker delta operator, and we absorbed the nonspatial derivatives into a new matrix $\mathbf{P}$. This matrix $\mathbf{P}$ is also the Jacobian of the corresponding nonspatial system [Eq. (8)]. The system is stable with respect to a given eigenperturbation if all eigenvalues of the corresponding Jacobian have negative real parts. The homogeneous steady state is thus stable if all the eigenmodes are stable, i.e., if the eigenvalues of $\mathbf{J}$ are negative for all wave numbers κ_n. We speak of a diffusion-driven instability when a change of parameters leads to the appearance of eigenvalues with positive real part for at least one nonzero wave number κ_n.

IV. DIFFUSION-DRIVEN INSTABILITIES IN NETWORKS

The beauty of the well-established method for the analysis of diffusion-driven instabilities, revisited above, is that the spatial (formally infinite-dimensional) system can be analyzed by considering the Jacobian matrix for the corresponding nonspatial system with some simple additional terms $c\kappa_n$ added to the diagonal elements.

We now present a derivation that shows that in the network system a similar, equally elegant and equally simple, approach is possible in which one can obtain the stability of spatial modes on the underlying geographical network by analyzing the Jacobian of the corresponding nonspatial system and then adding a minor modification that accounts for the nature of the eigenmode under consideration.

As we now have to deal with two networks, the network of interactions between species and the underlying geographical network across which the agents diffuse we will avoid using the term "node" and instead use species to refer to a node of the species network and patch to refer to a node of the geographical network.

Consider a reaction-diffusion system on a network where X_{ia} is the concentration of agents of species a on patch i. The dynamics of the system is captured by the equation

$$\dot{X}_{ia} = \underbrace{f_a(\boldsymbol{X_i})}_{\text{reactions}} \underbrace{- \sum_j c_a L_{ij} X_{ja}}_{\text{diffusion}}, \qquad (12)$$

where f_a is a function describing the impact of reactions on species a depending on the local concentrations $\boldsymbol{X_i} = (X_{i1}, \ldots, X_{iM})$, c_a is the diffusion constant for species a, and $\mathbf{L}$ is again the Laplacian matrix. This equation, Eq. (12), is the network analog of the continuous space equation (7).

For comparison, we also consider the corresponding nonspatial system

$$\dot{X}_a = f_a(\boldsymbol{X}). \qquad (13)$$

For any given stationary state $\boldsymbol{X}^*$ of Eq. (13) we can construct a homogeneous state of the network system (12):

$$X_{ia}{}^* = X_a{}^* \quad \forall\, i. \qquad (14)$$

We can quickly verify that the homogeneous states constructed in this way are stationary states of Eq. (12) because X_{ia}^* satisfies $f_a(\boldsymbol{X_i}) = 0$ for all i by construction. Furthermore, due to the zero row sum of the Laplacian it is true that $\mathbf{L}\boldsymbol{X_a} = 0$ for all vectors $\boldsymbol{X_a} = (X_{1,a}, \ldots, X_{N,a})$, where $X_{1,a} = \cdots = X_{N,a}$.

Thus, every stationary state of the nonspatial system corresponds to a stationary homogeneous state of the network system. This statement is the network's analog of the statement from our second bullet point in the previous section.

In the final, but most important, step we now show that the stability of the homogeneous states can also be analyzed analogously to the continuous space system, i.e., we can find the stability of network system by writing a Jacobian matrix that is identical to the Jacobian of the nonspatial system except for a minor modification. Analogously to the continuous case, this modification depends on the "wave number" under

consideration, i.e., the eigenvalue of the respective Laplace operator.

The network reaction-diffusion system is a large (i.e., NM-dimensional) dynamical system. We can therefore analyze its stability by constructing the corresponding Jacobian matrix $\mathbf{J}$. To do this, we must first bring the variables in linear order in a new vector

$$\boldsymbol{Y} = (X_{1,1}, \ldots, X_{1,M}, X_{2,1}, \ldots), \tag{15}$$

i.e., we order the variables such that the variables for all species in a given patch stay together. We can then compute the Jacobian matrix as

$$J_{lm} = \left. \frac{\partial}{\partial Y_m} \dot{Y}_l \right|_*. \tag{16}$$

This matrix has the block structure illustrated in Fig. 1. We show this by computing the derivatives of the reaction and the diffusion terms separately [cf. Eq. (12)]. The reaction rates at a given patch depend only on the concentrations in that patch. Therefore, they vanish when differentiated with respect to concentrations in a different patch

$$\frac{\partial}{\partial X_{jb}} f_a(\boldsymbol{X_i}) = 0 \quad \forall\, i \neq j. \tag{17}$$

The derivative of a reaction term with respect to a variable in the same patch is identical to the corresponding derivative in the nonspatial system [Eq. (13)]

$$\left. \frac{\partial}{\partial X_{ib}} f_a(\boldsymbol{X_i}) \right|_* = P_{ab}. \tag{18}$$

The contribution of the reaction terms to the Jacobian of the network system therefore has the form

$$\begin{pmatrix} \mathbf{P} & 0 & 0 & \cdots \\ 0 & \mathbf{P} & 0 & \cdots \\ 0 & 0 & \mathbf{P} & \cdots \\ \vdots & \vdots & \vdots & \ddots \end{pmatrix} \equiv \mathbf{I} \otimes \mathbf{P},$$

where $\otimes$ denotes the Kronecker product. The identity matrix used here has a linear dimension equal to the number of patches N, while the 0 and $\mathbf{P}$ matrices have a linear dimension equal to the number of species M.

Let us now consider the diffusion terms. Since we have assumed simple diffusion with a diffusion term that is linear in the concentration, we obtain directly

$$\left. \frac{\partial}{\partial X_{jb}} \sum_k c_a L_{ik} X_{ka} \right|_* = c_a L_{ij} \left. \frac{\partial}{\partial X_{jb}} X_{ja} \right|_* \equiv (\mathbf{L} \otimes \mathbf{C})_{ia,jb} \tag{19}$$

with

$$\mathbf{C} = \begin{pmatrix} c_1 & 0 & 0 & \cdots \\ 0 & c_2 & 0 & \cdots \\ 0 & 0 & c_3 & \cdots \\ \vdots & \vdots & \vdots & \ddots \end{pmatrix}.$$

In the following, we will lift the restriction to simple diffusion, where the matrix $\mathbf{C}$ is diagonal. In certain applications, the rates of diffusion can be a function of the concentrations of agents of the considered species and other species at the source. For example, in an ecological context this allows to model animals that leave a patch more quickly in response to overcrowding when food is scarce or when predators are abundant in a patch. When we make again a linear approximation around the steady state, the diffusion term in Eq. (12) takes in this case the more general form

$$-\sum_{j,b} c_{ab} L_{ij} X_{jb}. \tag{20}$$

Now, the coefficients c_{ab} become the elements of the matrix $\mathbf{C}$.

Summarizing the above, we can write the Jacobian of the network system in the compact form

$$\mathbf{J} = \mathbf{I} \otimes \mathbf{P} - \mathbf{L} \otimes \mathbf{C}. \tag{21}$$

The construction of the Jacobian from the different matrices is illustrated in Fig. 1.

Because the matrix has a block structure, a similar structure exists in its eigenvectors. Consider vectors constructed as

$$\boldsymbol{w} = \boldsymbol{v} \otimes \boldsymbol{q}, \tag{22}$$

where $\boldsymbol{v}$ is an N-dimensional vector and $\boldsymbol{q}$ is an M-dimensional vector. Now, let $\boldsymbol{v}$ be an eigenvector of $\mathbf{L}$ with eigenvalue κ such that

$$\mathbf{L}\boldsymbol{v} = \kappa \boldsymbol{v}. \tag{23}$$

Furthermore, let $\boldsymbol{q}$ be an eigenvector of $\mathbf{P} - \kappa\mathbf{C}$ with the eigenvalue λ. Then, $\boldsymbol{w}$ is an eigenvector of $\mathbf{J}$ to the eigenvalue λ, as the following calculation shows:

$$\begin{aligned} \mathbf{J}\boldsymbol{w} &= (\mathbf{I} \otimes \mathbf{P} - \mathbf{L} \otimes \mathbf{C}) \cdot (\boldsymbol{v} \otimes \boldsymbol{q}) \\ &= (\mathbf{I} \otimes \mathbf{P}) \cdot (\boldsymbol{v} \otimes \boldsymbol{q}) - (\mathbf{L} \otimes \mathbf{C}) \cdot (\boldsymbol{v} \otimes \boldsymbol{q}) \\ &= \mathbf{I}\boldsymbol{v} \otimes \mathbf{P}\boldsymbol{q} - \mathbf{L}\boldsymbol{v} \otimes \mathbf{C}\boldsymbol{q} \\ &= \boldsymbol{v} \otimes \mathbf{P}\boldsymbol{q} - \kappa \boldsymbol{v} \otimes \mathbf{C}\boldsymbol{q} \\ &= \boldsymbol{v} \otimes (\mathbf{P} - \kappa\mathbf{C})\boldsymbol{q} \\ &= \boldsymbol{v} \otimes \lambda \boldsymbol{q} = \lambda(\boldsymbol{v} \otimes \boldsymbol{q}) = \lambda \boldsymbol{w}. \end{aligned} \tag{24}$$

As all eigenvectors of $\mathbf{J}$ can be constructed in this way, we can compute the complete spectrum of the network-level Jacobian as

$$\mathrm{Ev}(\mathbf{J}) = \bigcup_{n=1}^{N} \mathrm{Ev}(\mathbf{P} - \kappa_n \mathbf{C}), \tag{25}$$

which enables us to analyze the stability of the network reaction-diffusion system by first computing the spectrum of the Laplacian matrix (the network analog of wave numbers κ in the spatial domain and then computing the eigenvalues of $\mathbf{P} - \kappa\mathbf{C}$, i.e., by diagonalizing a matrix which is identical to the nonspatial Jacobian matrix $\mathbf{P}$ plus a minor modification $-\kappa\mathbf{C}$, which is specific to the respective eigenperturbation under consideration. In this sense, Eq. (25) establishes that diffusive instabilities in reaction-diffusion systems on networks can be computed using an approach that is analogous to the widely used approach to reaction-diffusion systems in continuous space.

In summary, there exists a deep analogy between diffusion in continuous space and diffusion in networks. Above, we

have shown that this analogy extends to diffusion-driven instabilities. In the network context, the negative Laplacian matrix $-\mathbf{L}$ takes the role of the Laplace operator in continuous space. Correspondingly, in the analysis the eigenvalues and eigenfunctions of the Laplace operator are replaced by the eigenvalues and eigenvectors of the Laplacian matrix. Analyzing diffusive instabilities is therefore not more complicated than analyzing those instabilities in continuous space. However, as networks tend to have more complex spectra, more complex behavior can be expected.

V. META-FOOD-WEB MODEL

In order to illustrate the power of this approach, we consider the example of a state-of-the-art meta-food-web model from ecology, consisting of a set of identical local food webs, coupled in a spatial network (see Fig. 1).

We build on the so-called generalized food-web model. This fairly complex fully nonlinear model has been derived originally in [41] and was used and validated in several recent ecological papers, e.g., [28,47]. While we refer the reader to [41,48] for a full discussion of the model, let us revisit some of the design principles, before we extend the model to a spatial context.

Consider a general system in which there is a population X that is subject to a gain G and a loss L. Without knowing further details of the gain and loss processes, we can model the system by

$$\dot{X} = G(X) - L(X), \tag{26}$$

where G and L are unspecified functions. Let us now assume that the system has a steady state X^*. This assumption is generally warranted in the sense that Eq. (26) defines a space of plausible models based on the available information. For every given X^* we can find a specific model within this space that has X^* as a steady state [49].

We can now define a normalized variable $x = X/X^*$ and normalized functions $g(x) = G(X)/G(X^*)$, $l(x) = L(X)/L(X^*)$, which allow us to rewrite Eq. (26) as

$$\dot{x} = \alpha[g(x) - l(x)], \tag{27}$$

where $\alpha = G^*/X^* = L^*/X^*$. In the normalized system, the stationary state under consideration is $x^* = 1$ and its stability is determined by the Jacobian

$$\mathbf{P} = \alpha(\gamma - \mu), \tag{28}$$

where

$$\gamma = \frac{\partial}{\partial x} g(x)\bigg|_1 = \frac{\partial}{\partial \log X} \log G(x)\bigg|_*, \tag{29}$$

and μ is the corresponding derivative for L.

The advantage of writing the Jacobian in this way is that all the parameters that appear have an intuitive interpretations. The parameter α is a turnover rate and defines the time scale of the system. The parameters μ and γ are logarithmic derivatives, also called elasticities, which have advantageous statistical properties [50]. Moreover, for any power law, the corresponding elasticity is the exponent of the power law, e.g., linear losses imply $\mu = 1$ and quadratic losses imply $\mu = 2$.

The generalized model gives us analytical access to a convenient Jacobian that describes a broad class of systems. For instance, the Jacobian for the small example, Eq. (28), shows that in every system of that form, a given steady state is stable if the elasticity of loss in the steady state is greater than the elasticity of gain. The generalized food-web model extends the single-species case to a set of populations $X_1, \ldots, X_M$ described by

$$\dot{X}_a = G_a(X_a) - M_a(X_a) + \epsilon_a F_a(X_a, T_a(\boldsymbol{X})) - \sum_b \frac{R_{ab}(A_a, \boldsymbol{X})}{T_b(\boldsymbol{X})} F_b(X_b, T_a(\boldsymbol{X})) =: z_a, \tag{30}$$

where we introduced z_a an abbreviation that is useful below, and G_a, M_a, F_a are the gain of species a due to primary production, the nonpredatory mortality of species a, and the total gain of species a from predation, respectively. The function R_{ab} is the amount of species a that is effectively available to predator of species b. Often, this is a linear function of X_a, where the constant of proportionality it describes depends on the ability of species a to capture individuals of species b. Finally,

$$T_a = \sum_b R_{ba} \tag{31}$$

is the total amount of prey effectively available to species a.

Equation (30) can be normalized along the lines laid out in the simple example. As a result, we obtain a $M \times M$ Jacobian matrix $\mathbf{P}$ with diagonal entries

$$P_{aa} = \alpha_a \Bigg[\tilde{\nu}_a \tilde{\delta}_a \phi_a + \tilde{\nu}_a \delta_a (\gamma_a \chi_{aa} \lambda_{aa} + \psi_a) - \tilde{\rho}_a \tilde{\sigma}_a \mu_a - \tilde{\rho}_a \sigma_a \left(\beta_{aa} \psi_a + \sum_c \beta_{ca} \lambda_{ca} \left[(\gamma_c - 1)\chi_{ca} + 1 \right] \right) \Bigg] \tag{32}$$

and nondiagonal entries

$$P_{ab} = \alpha_a \Bigg[\tilde{\nu}_a \delta_a \gamma_a \chi_{ab} \lambda_{ab} - \tilde{\rho}_a \sigma_a \left(\beta_{ba} \psi_b + \sum_c \beta_{ca} \lambda_{cb} (\gamma_c - 1) \chi_{cb} \right) \Bigg], \tag{33}$$

where the parameters appearing in these equations are elasticities and turnover parameters describing the biomass flow in the system. One can now either estimate these parameters for a given experimental system [47] or one can use the generalized model to generate plausible random food webs [48]. Here, we use the second alternative.

We use the so-called niche model to generate realistic food-web topologies [51]. This model randomly assigns a body mass to every species and then determines the feeding interactions based on these body masses. The generalized model parameters are then drawn from suitable distributions that are dependent on the position of the species in the food web and the body mass parameter. In this way, realistic feeding behavior and realistic so-called allometric scaling of certain parameters with the body mass can be incorporated in the model. In the past, considerable effort has gone into investigating the realistic

ranges and distributions [48] the full parameters sets used in this paper are reproduced in the Appendix, and longer discussions of the parameters and their interpretation can be found in [41,48,52].

In this paper, we extend the generalized food-web model to a meta-food-web context. We consider a system consisting of N distinct habitat patches, where the dynamics within each patch i is given by the right-hand side of Eq. (30), abbreviated by z_a. Additionally, the populations are subject to spatial dispersal, modeled as a diffusion process on the network.

For clarity, we now use superscript indices i,j to denote the spatial patch while we continue to use subscript indices a,b,c to denote the species. Using this convention we can write the equations of motion as

$$\dot{X}_a^i = z_a(\boldsymbol{X}^i) + \sum_j \left[E_a^{ij}(\boldsymbol{X}^i) - E_a^{ji}(\boldsymbol{X}^i)\right], \tag{34}$$

where E_a^{ij} is the emigration rate of individuals of species a from patch j to patch i. These equations constitute the generalized meta-food-web model that is our example system in this paper.

By normalizing, linearizing, and then identifying elasticities and turnover rates, we can express the Jacobian matrix as a function of interpretable parameters. We note that this procedure can be applied to the reaction and the diffusion parts of the equation independently. For the reaction part, the procedure is completely analogous to nonspatial generalized food-web model that we discussed above. For the diffusion part, the treatment is analogous to the example of the reaction-diffusion system in Sec. II. In particular, the matrix $\mathbf{C}$ is obtained by taking the derivative of the (normalized) emigration term with respect to the (normalized) concentrations

$$A^{ij}C_{ab} = \left.\frac{\partial \log E_a^{ij}}{\partial \log X_b^i}\right|_*, \tag{35}$$

with the adjacency matrix $\mathbf{A}$. For normal diffusion, $\mathbf{C}$ is a diagonal matrix where C_{aa} is the diffusion constant of species a, however, for more complex cases such as cross diffusion, where predators leave preferentially if prey is low or prey flees if there are too many predators, it contains nondiagonal terms (see Sec. II). We present the detailed derivation in the Appendix.

In summary, the $(NM \times NM)$-dimensional Jacobian matrix of the generalized meta-food-web model can be written in the form (21):

$$\mathbf{J} = \mathbf{I} \otimes \mathbf{P} - \mathbf{L} \otimes \mathbf{C}. \tag{36}$$

For the present model, the matrix $\mathbf{P}$ is the Jacobian matrix of the nonspatial meta-food-web model [Eqs. (32) and (33)], $\mathbf{L}$ is the (possibly weighted) Laplacian of the underlying geographical network, and $\mathbf{C}$ is given by Eq. (35). (See also Fig. 1 for illustration.)

VI. DIFFUSION-DRIVEN INSTABILITIES IN META-FOOD WEBS

The previous section showed that the generalized meta-food-web model falls in the class of systems to which the results from Sec. IV apply. We can thus compute the eigenvalues using the formula in Eq. (25).

Equation (25) has the useful property that the structure of the spatial networks only enters through the eigenvalues. One can say that every Laplacian eigenvalue κ_i generates a set of Jacobian eigenvalues that is independent of the other Laplacian eigenvalues. This means that Eq. (25) defines a master stability function: Given only information about the local system (i.e., $\mathbf{P}$ and $\mathbf{C}$), we can compute the leading eigenvalue $\lambda_{\max}$ that would be generated by a given Laplacian eigenvalue κ [6,7]. The resulting function $S(\kappa) = \mathrm{Re}[\lambda_{\max}(\kappa)]$ is then a master stability function for the meta-food web under consideration.

Because stability requires all eigenvalues of the Jacobian to have negative real parts, stability is lost if any Laplacian eigenvalue falls into a range where the master stability function is positive. In the following, we refer to these ranges as "forbidden" as they have to be avoided if local stability is to be maintained. The loss of stability that occurs when eigenvalues enter these regions is analogous to the onset of pattern formation (Turing bifurcations, and wave instabilities) in continues space.

A. Stability of small food webs

Let us first consider the stability properties of the 4-species food web from Fig. 1. The master stability function corresponding to this food web is plotted in Fig. 3. Because the function only depends on the local network and the nature of the coupling, it is independent of the underlying spatial network into which the food web is placed. However, different spatial networks have different Laplacian spectra and thus sample the master stability function at different points, leading to different stability properties.

Linking the stability properties of the food web to Laplacian eigenvalues is interesting because the dependence of Laplacian spectrum on the topology of the network is relatively well understood [43]. The master stability function thus offers an opportunity to understand how the stability of network reaction-diffusion systems, or its loss, depends on topological properties.

The Laplacian matrix is a positive semidefinite matrix that always contains at least one zero eigenvalue. Hence, the spectrum of $\mathbf{J}$ always contains the set of eigenvalues generated by $\kappa = 0$, which are also the eigenvalues of $\mathbf{P}$. This shows that the homogeneous state in the meta-food web can only be stable if the corresponding steady state in the nonspatial food web is stable.

We numerically computed the MSF for a variety of randomly generated food webs. In smaller webs with up to five species, we mostly observed MSFs with relatively simple shapes, where the MSF is either (i) positive at zero, (ii) negative everywhere, or (iii) crosses from negative to positive values at a single $\kappa^* > 0$ (cf. Fig. 3). The former two cases correspond to food webs that are unstable (i) or stable (ii) irrespective of the geographical network, whereas the third case (iii) is stable if all eigenvalues of the Laplacian are sufficiently small ($\kappa_i < \kappa^*$).

Uniformly increasing the diffusion constant in a given network stretches the Laplacian spectrum. In systems of class (iii), the homogeneous state is therefore at greater risk of instability in networks where the diffusive coupling is stronger. This shows that densely linked landscapes, which are thought to be beneficial in ecology, may lead to instability of the

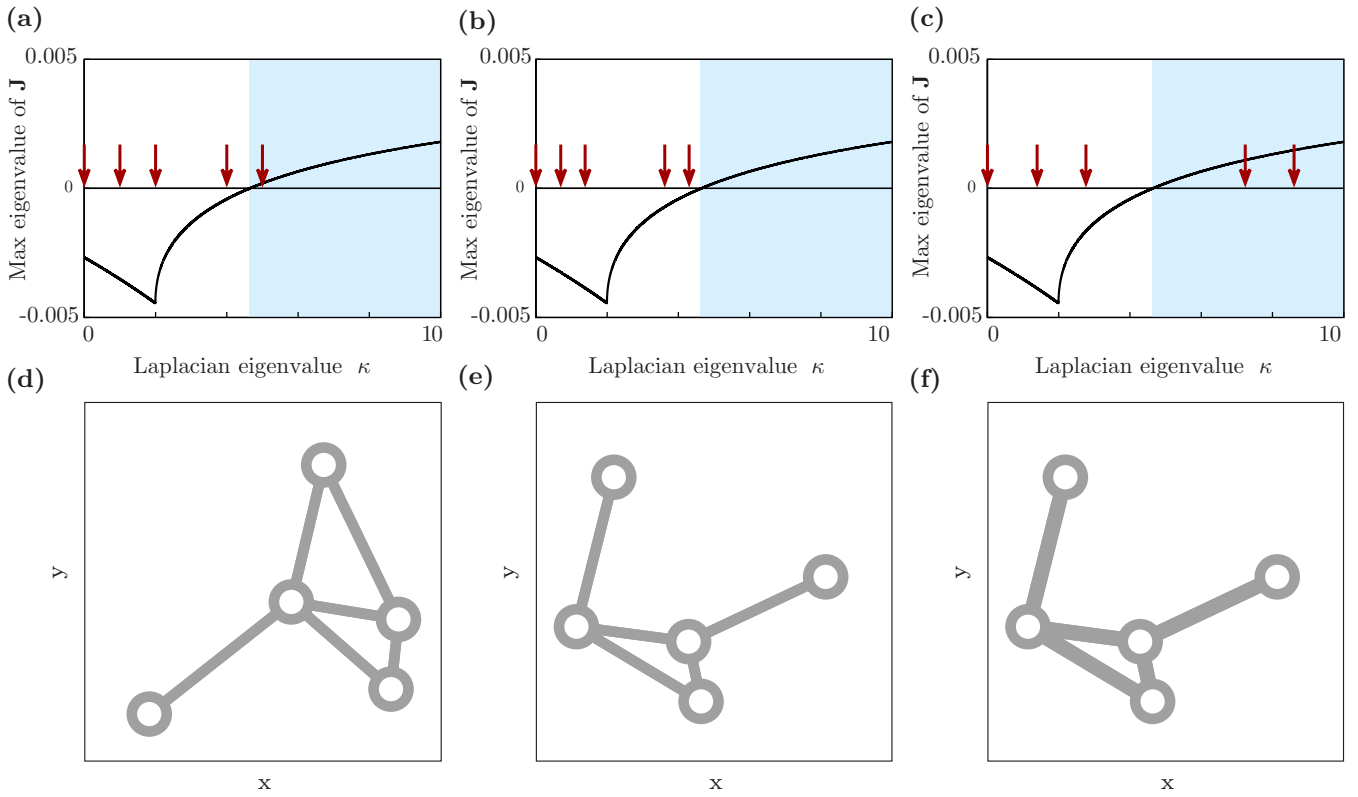

FIG. 3. Master stability function (MSF) for meta-food webs. Shown are MSFs (a)–(c) and spatial geometries (d)–(f) for the same local food web (that of Fig. 1) and coupling matrix **C** [see Eq. (36) and Appendix for details] but three different geometries (represented by circles, indicating patches, and lines, indicating migration links, in a two-dimensional x, y landscape). The MSF [identical line in (a)–(c)] relates the Jacobian eigenvalue of the meta-food web to the Laplacian eigenvalue of the spatial network. The meta-food web is stable if none of the Laplacian eigenvalues (arrows) fall into ranges where the master stability function [line in (a)–(c)] is positive (blue shaded area). The food web under consideration is unstable on one geometry (a), (d) but stable on another (b), (e). Tightening the coupling, i.e., increasing the weights in the adjacency matrix [indicated by thicker lines in (f)], can destabilize the stable system by stretching the Laplacian spectrum [cf. (b) and (c)].

homogeneous steady state in a food web of class (iii). However, this instability is not necessarily detrimental as it can lead to stable spatial patterns that introduce heterogeneity, which might ultimately benefit the diversity of the system [53].

B. Stability of larger food webs

The analysis of small food webs, including the example in Fig. 3, revealed relatively simple master stability functions, which are very similar to the master stability functions observed in coupled oscillator models. However, in large food webs and particularly if cross diffusion is allowed, much more complex functions can be observed.

Figure 4 shows two examples of 30-species meta-food webs and their corresponding master stability functions. The functions go through a complex pattern of stable and unstable intervals that defies easy classification. One could now explore the transitions in which forbidden regions are created and vanish, but this analysis exceeds the scope of this paper.

For ecology, the complex master stability functions are sobering as they show that there cannot be any simple laws that govern the stability of these systems. The only exception is perhaps that we can say that in a sufficiently weakly coupled system the Laplacian eigenvalues always cluster around zero. Since the master stability function has to be a continuous function there will always be a critical threshold for the coupling strength below which the stability properties of the weakly coupled system are identical to the stability properties of an isolated system.

In absence of easy rules for the stability of meta-food webs, ecologists will have to consider different food webs and different spatial networks individually. We believe that the methodology proposed here will prove conducive to this task.

C. Network spectra and localized modes

Throughout most of this paper we have argued that extensive analogies exist between reaction-diffusion systems in space and reaction-diffusion systems on networks. However, differences exist in the spectrum of the respective Laplacian operators.

In continuous spatial domains, the spectrum of the Laplacian operator tends to be relatively regular and the eigenmodes are typically delocalized functions such as trigonometric or Bessel functions. By contrast, the spectrum of the Laplace operator on networks has a complex structure, and the majority of eigenmodes are localized [54–56].

For illustration, we consider the well-studied example of random geometric graphs [57], which provide a generic model for spatial networks. They consist of nodes that are randomly

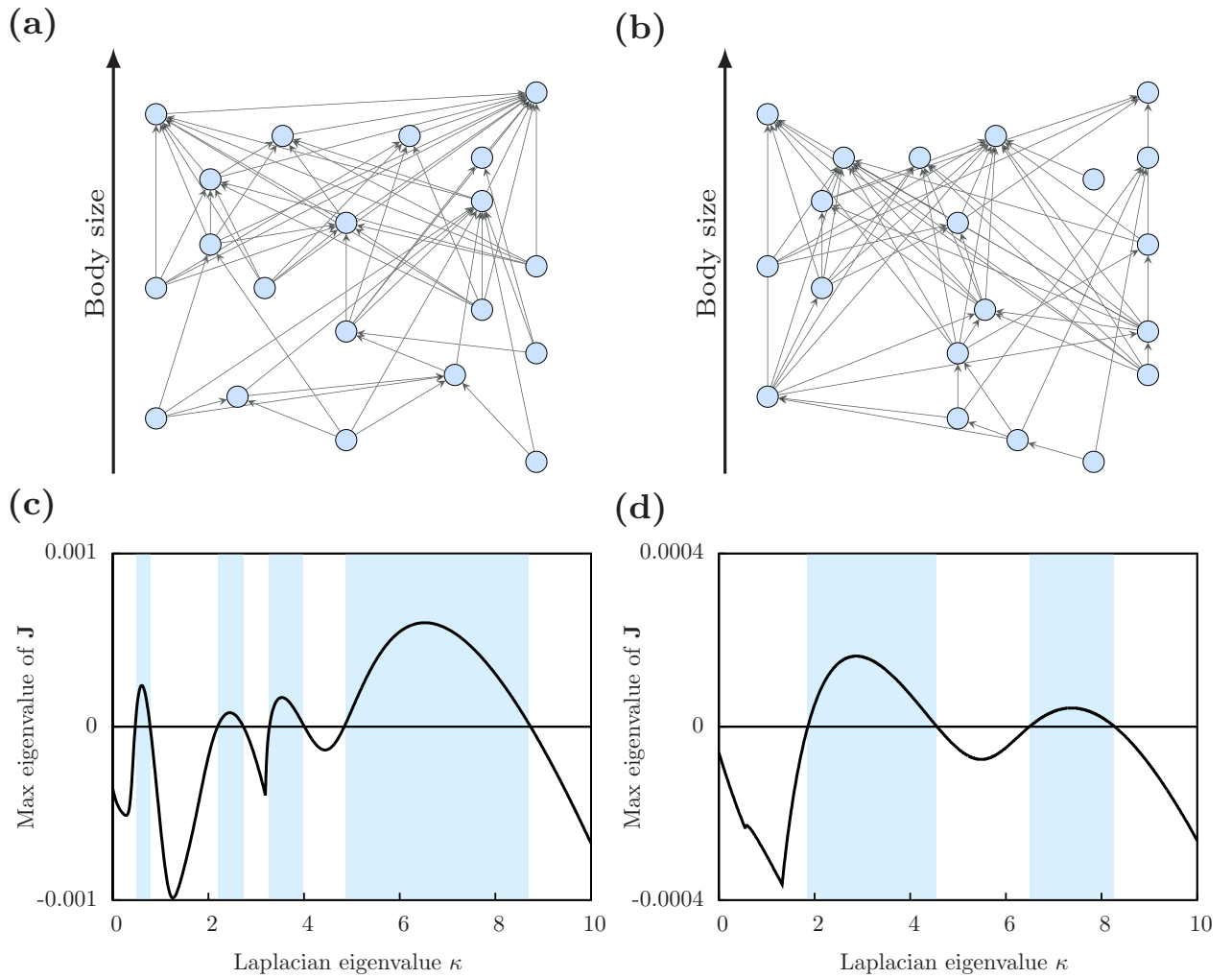

FIG. 4. Complex master stability functions (MSFs). Shown are two examples of food webs (a), (b) of 20 species (blue bubbles) connected by predator-prey interactions (arrows). The coupling matrix **C** was constructed such that predators emigrate preferentially from patches with scarce prey and prey emigrates preferentially from patches with abundant predators (see Appendix). The corresponding MSFs [(c) for (a), (d) for (b)] have many forbidden (blue) ranges.

placed in a square and that are connected to all neighbors within a certain distance. The extent to which an eigenvector is localized can be quantified by the participation number [55] which indicates the approximate number of nodes on which the eigenvector has a significant amplitude. In an example system of 500 spatial patches we find that more than 150 modes have a participation number of less than 10 and more than 200 additional modes have a participation number between 10 or 20 (Fig. 5). Thus more than half of the eigenvectors are localized on small clusters that contain less than 4% of the nodes.

In the context of reaction-diffusion systems, localized spatial modes have two implications:

(i) The corresponding eigenvalue is only sensitive to the structure inside the cluster, and thus the eigenvalue is informative of local features in that cluster.

(ii) If the eigenvalue lies in one of the forbidden regions, such that it generates a dynamical instability, this instability will at least initially be confined to the cluster on which the corresponding eigenmode is localized.

These properties of networks may make it possible to engineer systems where the dynamics reacts sensitively to local topological properties, a possibility that we discuss briefly in the Conclusions.

D. Numerical validation and behavior in unstable regions

We checked the theoretical results numerically by numerical diagonalization of the Jacobian matrix and by simulating specific dynamical models, which yielded a perfect agreement. Furthermore, we noticed that in systems where the homogeneous state is unstable, the system often approaches heterogeneous steady state for which variables in the different nodes are closely predicted by the unstable eigenmode.

While the mathematics imply that the system leaves the unstable state in a direction corresponding to the leading eigenvector [58], we are not aware of a mathematical reason why the eigenvector should remain informative after this initial departure. In low-dimensional systems, one typically observes that the system approaches some other attractor that is far away

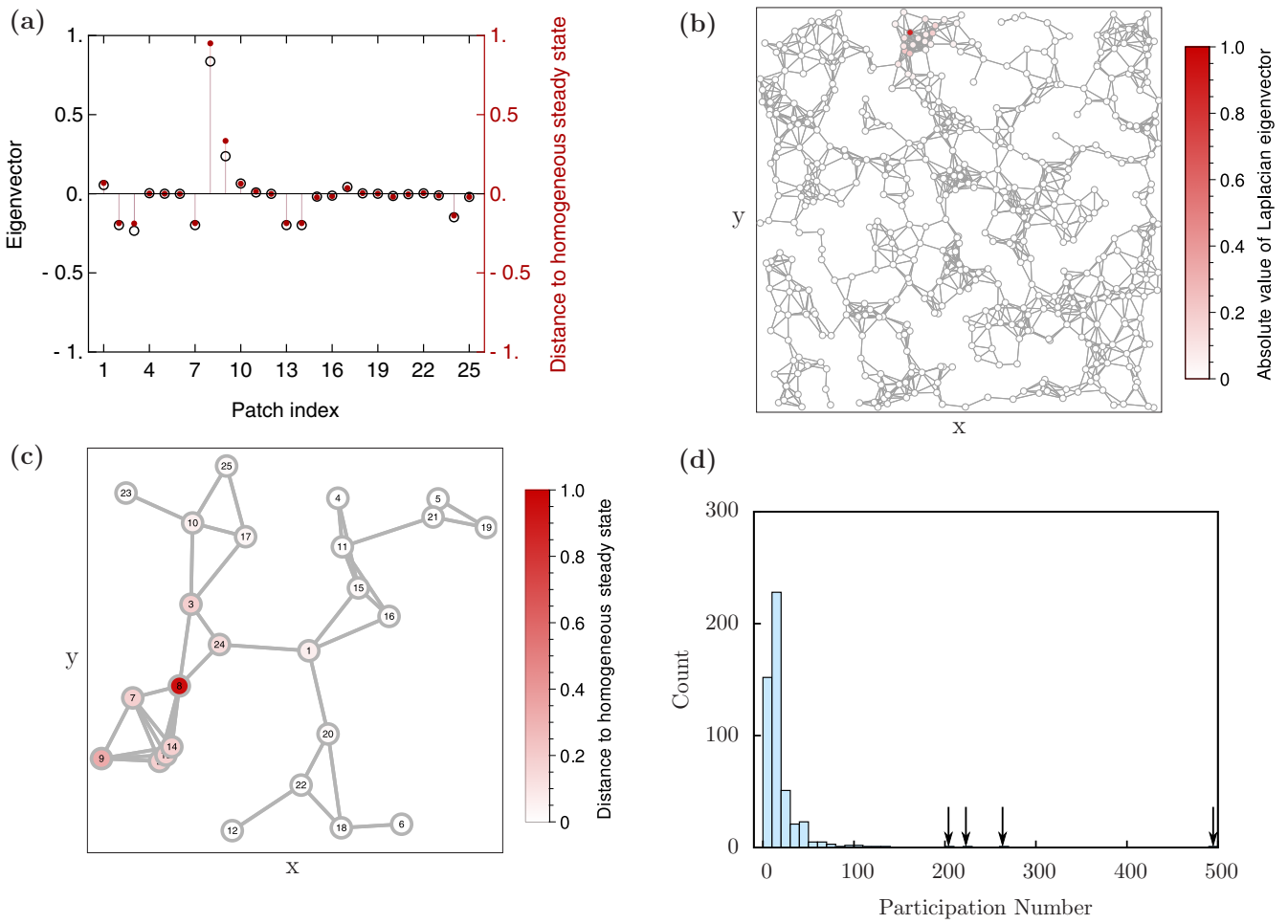

FIG. 5. Localization of eigenvectors. Shown is a system where on a given topology (c) one eigenvalue of the Laplacian lies in one of the forbidden ranges where the MSF of the food web is positive. Hence, the system departs from the homogeneous steady state and approaches a nonhomogeneous state. Color coding the distance of the density of the apex predator population to the homogeneous value (see methods) shows that the impact of the instability is confined to a relatively small area. In cases where the system approaches a state in the vicinity of the homogeneous state, the eigenvector corresponding to the destabilizing eigenvector is indicative of the pattern in the final state. A comparison (a) of the respective eigenvector (open circles) and the observed deviation from the homogeneous value in the final state (dots) shows good agreement in the example system (c), but similar accuracy cannot be guaranteed in general. The localization of many eigenvectors is a generic feature of geographical networks. For the 500-node example geometry in (b) the number of nodes on which eigenvectors have a significant amplitude can be quantified by the participation number (see methods). This reveals that the majority of eigenvectors only extend to relatively few nodes [histogram in (d)], while only four eigenvalues (arrows) have significant amplitude on a large fraction of the nodes. The example shown here is a case of real eigenvalues causing a Turing instability. When the leading eigenvalue is complex, the associated instability is a wave instability (see Appendix).

from the unstable state. While such catastrophic departures also occur in the network reaction-diffusion systems studied here, we also observed a large proportion of simulation runs where the developing pattern closely resembled the unstable eigenmode (see Fig. 5 for an example, and video linked in the Appendix).

VII. CONCLUSIONS

In this paper, we have shown that a deep analogy exists between reaction-diffusion system in continuous space and reaction-diffusion system on networks. The analysis of pattern forming diffusion-driven instabilities in networks is thus not more difficult than the analysis of such instabilities in continuous space, perhaps even easier as eigenmodes of large networks are easier to compute than eigenfunctions of complex spatial domains. Yet, networks have often a more complex spectrum including localized modes which can give rise to localized patterns.

Our analysis, while relying on Kronecker products, leads to a formulation that constitutes a master stability function. Given the long tradition that the master stability approach has in synchronization and the many modern applications, it is surprising that the application to stationary states proposed here has not been used in a wide range of applications already. In our opinion, there is plenty of untapped potential to leverage this approach for progress in applications.

Reaction-diffusion systems on networks can be described as multilayer networks, a class of systems that has recently gained much attention. Compared to other multilayer systems,

the networks studied here fall into a comparatively tame class as the layers are topologically identical. However, even with this restriction network reaction-diffusion systems can accommodate a high degree of complexity. We illustrated this point by analyzing the generalized meta-food-web model. This model described a set of species which have different nonlinear dynamics reflecting their different biology.

Although we required that all populations disperse over the same spatial network, diffusion can take place at different rates, which can moreover depend dynamically on the local conditions. Our analysis of small food webs revealed that in a broad class of system, tight spatial coupling can destabilize the homogeneous stationary states leading to pattern formation.

We also showed that large food webs can have very complex master stability functions, such that there cannot be any easy laws governing the stability of homogeneous states in these systems. This implies that systems from applications have to be studied separately in detail, and thus efficient approaches, such as the one proposed here, are needed.

We emphasize that the approach proposed here is not limited to the analysis of food webs. Let us therefore conclude by outlining other possible applications in biology:

(i) In game theory, network effects have been prominently discussed for some time. Using the proposed approach, population dynamical models, say of cooperator and defector populations, could be studied to determine under which conditions the state where agents are distributed homogeneously across the network becomes unstable creating patterns where havens for cooperators exist.

(ii) In epidemiology, stability analysis of homogeneous disease free states have been proposed as a method to compute epidemic thresholds for a single pathogen. However, there is a significant interest in coinfection models using multiple microbes. Using the proposed approach, master stability functions for the invasion of large microbial communities could be computed, providing insights into transmission of microbiomes. In this application, the adjacency matrix replaces the Laplacian as the spatial operator, but the approach can be straightforwardly extended to accommodate this matrix.

(iii) In cell biology, the approach could be used to investigate the dynamics tissues of identical cells. Particularly, one could ask how metabolic or signaling interactions could lead to pattern formation. In the context synthetic biology the abundance of localized eigenmodes in spatial networks might be exploited to engineer reaction systems for which pattern formation localizes on certain topological features, e.g., detecting for example areas in the tissue where cells are particularly highly clustered.

We hope that the approach proposed here will be conducive to advancing the understanding in these and other applications.

ACKNOWLEDGMENTS

We thank Dr. L. Rudolf for help with the generation of generalized niche model webs. This work was supported by DFG Projects No. Dr300/12-2 and No. Dr300/13-2 and EPSRC Projects No. EP/K031686/1 and No. EP/N034384/1. It was also financially supported in part by Perimeter Institute for Theoretical Physics. Research at Perimeter Institute is supported by the Government of Canada through the Department of Innovation, Science and Economic Development Canada and by the Province of Ontario through the Ministry of Research, Innovation and Science.

Data statement. In compliance with EPSRC policy framework on research data, we confirm that this work did not produce or use primary research data.

A.B., P.G., D.R. contributed equally to this work, and B.D. and T.G. contributed equally to this work.

APPENDIX

1. Full generalized meta-food-web model

We denote the biomass density of species i in habitat k by X_i^k. Its change is given by

$$\begin{aligned}\dot{X}_i^k = {} & G_i^k\big(X_i^k\big) - M_i^k\big(X_i^k\big) + \epsilon_i F_i^k\big(X_1^k,\ldots,X_S^k\big) \\ & - \sum_j D_{ji}^k\big(X_1^k,\ldots,X_S^k\big) \\ & + \sum_l \big[E_i^{kl}\big(X_1^k,\ldots,X_S^k,X_1^l,\ldots,X_S^l\big) \\ & - E_i^{lk}\big(X_1^l,\ldots,X_S^l,X_1^k,\ldots,X_S^k\big)\big], \end{aligned} \tag{A1}$$

where G_i^k is the growth by primary production, M_i^k is the loss by respiration and mortality, F_i^k is the growth due to predation, D_{ji}^k is the loss of biomass due to predation by species j, E_i^{kl} is the migration from habitat l to k. Furthermore, we used ϵ_i to denote the conversion efficiency of prey biomass.

Following Gross *et al.* [41] we capture the correlation between the loss of the prey species D_{ji}^k and the growth of the corresponding predators F_j^k, by introducing the auxiliary variable for the total amount of prey that is available to species j in habitat k,

$$T_j^k\big(X_1^k,\ldots,X_S^k\big) = \sum_i R_{ji}^k\big(X_i^k\big), \tag{A2}$$

where $R_{ji}^k(X_i^k)$ is the relative contribution of species i in patch k to the total amount of food available to the population of species j in the habitat.

We can now write the amount of prey consumed by population j as

$$F_j^k\big(X_1^k,\ldots,X_N^k\big) = F_j^k\big(T_j^k,X_j^k\big), \tag{A3}$$

and the loss of species i due to predation by species j in habitat k as

$$D_{ji}^k\big(X_1^k,\ldots,X_S^k\big) = \frac{R_{ji}^k\big(X_i^k\big)}{T_j^k\big(X_1^k,\ldots,X_S^k\big)} F_j^k\big(T_j^k,X_j^k\big). \tag{A4}$$

2. Derivation of Jacobian matrix

We assume that the system in Eq. (A1) has at least one positive (but potentially unstable) steady state. This is a very mild assumption, given the considerable freedom that still exists in the class of models. We then denote the (unknown) steady-state population densities by X_i^{k*}. Likewise, we use the asterisk to denote functions evaluated in the steady state, e.g., $F_i^{k*} = F_i^k(X_1^{k*},\ldots,X_S^{k*})$. We then normalize all dynamical variables and functions by their steady-state value. The results

of this normalization are denoted by lowercase symbols For instance, $x_i^k = \frac{X_i^k}{X_i^{k*}}$.

Using these definitions we obtain the normalized equations

$$\begin{aligned}\dot{x}_i^k = {} & \frac{G_i^{k*}}{X_i^{k*}} g_i^k\left(x_i^k\right) - \frac{M_i^{k*}}{X_i^{k*}} m_i^k\left(x_i^k\right) + \frac{\epsilon_i F_i^{k*}}{X_i^{k*}} f_i^k\left(t_i^k, x_i^k\right) \\ & - \sum_j \frac{D_{ji}^{k*}}{X_i^{k*}} d_{ji}^k\left(x_1^k, \ldots, x_S^k\right) \\ & + \sum_l \left[\frac{E_i^{kl*}}{X_i^{k*}} e_i^{kl}\left(x_1^k, \ldots, x_S^k, x_1^l, \ldots, x_S^l\right) \right. \\ & \left. - \frac{E_i^{lk*}}{X_i^{k*}} e_i^{lk}\left(x_1^l, \ldots, x_S^l, x_1^k, \ldots, x_S^k\right) \right]. \end{aligned} \tag{A5}$$

We can now identify a set of structural parameters that characterize the biomass flow in the steady state under consideration. In the context of Generalized Model (GM) such parameters are called *scale parameters*. We start with the time scales

$$\begin{aligned}\alpha_i^k &= \frac{G_i^{k*}}{X_i^{k*}} + \frac{\epsilon_i F_i^{k*}}{X_i^{k*}} + \sum_l \frac{E_i^{kl*}}{X_i^{k*}} \\ &= \frac{M_i^{k*}}{X_i^{k*}} + \sum_j \frac{D_{ji}^{k*}}{X_i^{k*}} + \sum_l \frac{E_i^{lk*}}{X_i^{k*}}. \end{aligned} \tag{A6}$$

These scale parameters quantify the rate of biomass flow in the steady state. The relative contributions to the biomass gain by the different processes are

$$\nu_i^k = \sum_l \nu_i^{kl} = \frac{1}{\alpha_i^k} \sum_l \frac{E_i^{kl*}}{X_i^*}, \tag{A7}$$

$$\tilde{\nu}_i^k = 1 - \nu_i^k = \frac{1}{\alpha_i^k} \frac{\epsilon_i F_i^{k*}}{X_i^{k*}} + \frac{1}{\alpha_i^k} \frac{G_i^{k*}}{X_i^{k*}}, \tag{A8}$$

$$\tilde{\nu}_i^k \delta_i^k = \frac{1}{\alpha_i^k} \frac{\epsilon_i F_i^{k*}}{X_i^{k*}}, \tag{A9}$$

$$\tilde{\nu}_i^k \tilde{\delta}_i^k = \tilde{\nu}_i^k \left(1 - \delta_i^k\right) = \frac{1}{\alpha_i^k} \frac{G_i^{k*}}{X_i^{k*}}. \tag{A10}$$

The relative contributions of the different processes to the biomass loss are given by

$$\rho_i^k = \sum_l \rho_i^{lk} = \frac{1}{\alpha_i^k} \sum_l \frac{E_i^{lk*}}{X_i^*}, \tag{A11}$$

$$\tilde{\rho}_i^k = 1 - \rho_i^k = \frac{1}{\alpha_i^k} \frac{M_i^{k*}}{X_i^{k*}} + \frac{1}{\alpha_i^k} \sum_j \frac{D_{ji}^{k*}}{X_i^{k*}}, \tag{A12}$$

$$\tilde{\rho}_i^k \sigma_i^k = \frac{1}{\alpha_i^k} \sum_j \frac{D_{ji}^{k*}}{X_i^{k*}}, \tag{A13}$$

$$\tilde{\rho}_i^k \tilde{\sigma}_i^k = \tilde{\rho}_i^k \left(1 - \sigma_i^k\right) = \frac{1}{\alpha_i^k} \frac{M_i^{k*}}{X_i^{k*}}. \tag{A14}$$

It is necessary to resolve the contribution of different species to the loss by additionally defining the parameters

$$\beta_{ji}^k = \frac{1}{\alpha_i^k \tilde{\rho}_i^k \sigma_i^k} \frac{D_{ji}^{k*}}{X_i^{k*}}. \tag{A15}$$

Using Eq. (A4), the normalized function for the loss due to predation can be written as

$$\begin{aligned} d_{ji}\left(x_1^k, \ldots, x_S^k\right) &= \frac{R_{ji}^{k*} F_j^{k*}}{T_j^{k*} D_{ji}^{k*}} \frac{r_{ji}^k}{t_j^k} f_j\left(t_j^k, x_j^k\right) \\ &= \frac{r_{ji}^k}{t_j^k} f_j\left(t_j^k, x_j^k\right), \end{aligned} \tag{A16}$$

where the normalized total available biomass for predation by species j is given by

$$t_j^k = \sum_i \frac{R_{ji}^{k*}}{T_j^{k*}} r_{ji}^k. \tag{A17}$$

Using the parameters

$$\chi_{ji}^k = \frac{R_{ji}^{k*}}{T_j^{k*}}, \tag{A18}$$

we can write

$$t_j^k = \sum_i \chi_{ji}^k r_{ji}. \tag{A19}$$

In summary, this yields the normalized meta-food-web model

$$\begin{aligned}\dot{x}_i^k = \alpha_i^k \Bigg[& \tilde{\nu}_i^k \tilde{\delta}_i^k g_i^k\left(x_i^k\right) + \tilde{\nu}_i^k \delta_i^k f_i^k\left(t_i^k, x_i^k\right) - \tilde{\rho}_i^k \tilde{\sigma}_i^k m_i^k\left(x_i^k\right) \\ & - \tilde{\rho}_i^k \sigma_i^k \sum_j \beta_{ji}^k d_{ji}^k\left(x_1^k, \ldots, x_S^k\right) \\ & + \sum_l \nu_i^{kl} e_i^{kl}\left(x_1^k, \ldots, x_S^k, x_1^l, \ldots, x_S^l\right) \\ & - \sum_l \rho_i^{lk} e_i^{lk}\left(x_1^l, \ldots, x_S^l, x_1^k, \ldots, x_S^k\right) \Bigg], \end{aligned} \tag{A20}$$

where $i = 1, \ldots, S$ and $k = 1, \ldots, N$.

3. Calculation of the Jacobian

Our model still contains unknown functional forms. However, the only aspect of this uncertainty that is relevant for the local dynamics are certain derivatives of the functions evaluated in the unknown steady state under consideration. The core of GM is the idea that this uncertainty can be captured in so-called *exponent parameters*, which we define as

$$\phi_i^k = \left. \frac{\partial}{\partial x_i^k} g_i^k\left(x_i^k\right) \right|_{x=x^*}, \tag{A21}$$

$$\mu_i^k = \left. \frac{\partial}{\partial x_i^k} m_i^k\left(x_i^k\right) \right|_{x=x^*}, \tag{A22}$$

$$\lambda_{ji}^k = \left. \frac{\partial}{\partial x_i^k} r_{ji}^k\left(x_i^k\right) \right|_{x=x^*}, \tag{A23}$$

$$\gamma_i^k = \left. \frac{\partial}{\partial t_i^k} f_i^k\left(t_i^k, x_i^k\right) \right|_{x=x^*}, \tag{A24}$$

$$\psi_i^k = \left. \frac{\partial}{\partial x_i^k} f_i^k\left(t_i^k, x_i^k\right) \right|_{x=x^*}, \tag{A25}$$

and for migration

$$\hat{\omega}_i^{kl} = \frac{\partial}{\partial x_i^k} e_i^{kl}\left(x_1^k,\ldots,x_S^k,x_1^l,\ldots,x_S^l\right)\Big|_{x=x^*}, \tag{A26}$$

$$\omega_i^{kl} = \frac{\partial}{\partial x_i^l} e_i^{kl}\left(x_1^k,\ldots,x_S^k,x_1^l,\ldots,x_S^l\right)\Big|_{x=x^*}, \tag{A27}$$

$$\hat{\kappa}_{ij}^{kl} = \frac{\partial}{\partial x_j^k} e_i^{kl}\left(x_1^k,\ldots,x_S^k,x_1^l,\ldots,x_S^l\right)\Big|_{x=x^*} \quad \text{mit } i \neq j, \tag{A28}$$

$$\kappa_{ij}^{kl} = \frac{\partial}{\partial x_j^l} e_i^{kl}\left(x_1^k,\ldots,x_S^k,x_1^l,\ldots,x_S^l\right)\Big|_{x=x^*} \quad \text{mit } i \neq j. \tag{A29}$$

4. Matrix representation

We use three types of matrices to construct the Jacobian. The matrices $\mathbf{P}^k$ capture the local biology within a patch, whereas the matrices $\mathbf{C}^{kl}$ and $\hat{\mathbf{C}}^{kl}$ capture the dependencies caused by migration from patch l to k. From the GM above, we find the diagonal elements of $\mathbf{P}^k$:

$$P_{ii}^k = \alpha_i^k\Bigg[\tilde{\nu}_i^k\tilde{\delta}_i^k\phi_i^k + \tilde{\nu}_i^k\delta_i^k\left(\gamma_i^k\chi_{ii}^k\lambda_{ii}^k + \psi_i^k\right) - \tilde{\rho}_i^k\tilde{\sigma}_i^k\mu_i^k - \tilde{\rho}_i^k\sigma_i^k\left(\beta_{ii}^k\psi_i^k + \sum_n \beta_{ni}\lambda_{ni}\left[\left(\gamma_n^k - 1\right)\chi_{ni}^k + 1\right]\right)\Bigg], \tag{A30}$$

and the nondiagonal elements

$$P_{ij}^k = \alpha_i^k\Bigg[\tilde{\nu}_i^k\delta_i^k\gamma_i^k\chi_{ij}^k\lambda_{ij}^k - \tilde{\rho}_i^k\sigma_i^k\left(\beta_{ji}^k\psi_j^k + \sum_n \beta_{ni}^k\lambda_{nj}^k\left(\gamma_n^k - 1\right)\chi_{nj}\right)\Bigg]. \tag{A31}$$

The matrices $\mathbf{C}^{kl}$ have diagonal elements

$$C_{ii}^{kl} = \alpha_i^k\left[\rho_i^{lk}\omega_i^{lk} - \nu_i^{kl}\hat{\omega}_i^{kl}\right] \tag{A32}$$

and nondiagonal elements

$$C_{ij}^{kl} = \alpha_i^k\left[\rho_i^{lk}\kappa_{ij}^{lk} - \nu_i^{kl}\hat{\kappa}_{ij}^{lk}\right]. \tag{A33}$$

The analogously defined matrices $\hat{\mathbf{C}}^{kl}$ with swapped scale parameters have the diagonal elements

$$\hat{C}_{ii}^{kl} = \alpha_i^k\left[\nu_i^{lk}\omega_i^{lk} - \rho_i^{kl}\hat{\omega}_i^{kl}\right] \tag{A34}$$

and the nondiagonal elements

$$\hat{C}_{ij}^{kl} = \alpha_i^k\left[\nu_i^{lk}\kappa_{ij}^{lk} - \rho_i^{kl}\hat{\kappa}_{ij}^{kl}\right]. \tag{A35}$$

The Jacobian is then constructed as

$$\mathbf{J} = \begin{pmatrix} \ddots & & & \\ & \mathbf{P}^k - \sum_m \mathbf{C}^{km} & \cdots & \hat{\mathbf{C}}^{kl} \\ & \vdots & \ddots & \vdots \\ & \hat{\mathbf{C}}^{lk} & \cdots & \mathbf{P}^l - \sum_m \mathbf{C}^{lm} \\ & & & \ddots \end{pmatrix}. \tag{A36}$$

TABLE I. Generalized parameters used to describe the meta-food web. The indices i and j denote different species and k and l different habitats.

Parameter	Interpretation
Elasticity	
ϕ_i^k	Sensitivity of primary production of i in k to itself
γ_i^k	Sensitivity of predation of i in k to prey density
λ_i^k	Exponent of prey switching of i in k
ψ_i^k	Sensitivity of predation of i to density of itself
μ_i^k	Exponent of closure of i in k
ω_i^{kl}	Sensitivity of migration of i from l to k to itself
$\tilde{\omega}_i^{kl}$	Sensitivity of migration of i from l to k to itself
κ_{ij}^{kl}	Sensitivity of migration of i from l to k to j
$\tilde{\kappa}_{ij}^{kl}$	Sensitivity of migration of i from l to k to j
Turnover	
$\alpha_{P_i}^k$	Intrahabitat biomass flow of i in k
$\alpha_{C_i}^k$	Biomass flow by migration of i in k
β_{ji}^k	Contribution of predation by i to local biomass loss of j
σ_i^k	Fraction of local biomass loss of i in k due to predation
$\tilde{\sigma}_i^k$	Fraction of local biomass loss of i in k due to respiration
δ_i^k	Fraction of local growth by predation of i in k
$\tilde{\delta}_i^k$	Fraction of local growth by primary production of i in k
χ_i	Contribution of i to prey of j on k
ν_i^k	Fraction of total biomass gain of i in k due to migration
$\tilde{\nu}_i^k$	Fraction of total biomass gain of i in k due to predation
ρ_i^k	Fraction of total biomass loss of i in k due to migration
$\tilde{\rho}_i^k$	Fraction of total biomass loss of i in k due to predation
η_i^{kl}	Fraction of migration biomass flow of i due to migration from l to k

The unknown stable steady state under consideration is stable if all eigenvalues have negative real parts.

Although the functions and the steady states are unknown, the exponent and scale parameters that enter the Jacobian are directly interpretable in the context of the system and can therefore be measured directly in nature or can be chosen to based on theoretical considerations (see Gross *et al.* [28,41] and Table I for details).

Note that different steady states are characterized by different values of the scale and exponent parameters and thus can have different stability properties.

In the context of this paper, we consider the stability of homogeneous steady states, i.e., states in which all patches are characterized by the same parameters and have the same biomass density. We then speak of diffusion-driven instability (DDI) if such a state is stable without diffusion, but loses stability under nonzero diffusive coupling.

5. Diffusive mass balance in homogeneous states

For a homogeneous equilibrium, the incoming flux experienced by a given population must equal the outgoing flux

$$\tilde{\nu}_i^k\alpha_i^k = \tilde{\rho}_i^k\alpha_i^k \tag{A37}$$

and furthermore

$$\nu_i^k \alpha_i^k = \rho_i^k \alpha_i^k. \tag{A38}$$

Therefore, we obtain

$$\tilde{\nu}_i^k = \tilde{\rho}_i^k \tag{A39}$$

and

$$\nu_i^k = \rho_i^k. \tag{A40}$$

Thus, we define the local biomass flow

$$\alpha_{P_i}^k = \tilde{\nu}_i^k \alpha_i^k = \tilde{\rho}_i^k \alpha_i^k \tag{A41}$$

and the biomass flow due to migration

$$\alpha_{C_i}^k = \nu_i^k \alpha_i^k = \rho_i^k \alpha_i^k. \tag{A42}$$

At this point, we have to introduce the auxiliary scale parameters η_i^{kl} to keep track of the relative contributions of the spatial links to the migration bimass flow:

$$\nu_i^{kl} \alpha_i^k = \rho_i^{kl} \alpha_i^k = \eta_i^{kl} \alpha_{C_i}^k. \tag{A43}$$

Using these definitions, we can rewrite the matrices $\mathbf{P}^k$ and $\mathbf{C}^{kl} = \hat{\mathbf{C}}^{kl}$. The matrix for local dynamics is given by

$$P_{ii}^k = \alpha_{P_i}^k \Bigg[\tilde{\delta}_i^k \phi_i^k + \delta_i^k \left(\gamma_i^k \chi_{ii}^k \lambda_{ii}^k + \psi_i^k \right) - \tilde{\sigma}_i^k \mu_i^k - \sigma_i^k \left(\beta_{ii}^k \psi_i^k + \sum_n \beta_{ni} \lambda_{ni} \left[\left(\gamma_n^k - 1 \right) \chi_{ni}^k + 1 \right] \right) \Bigg] \tag{A44}$$

and

$$P_{ij}^k = \alpha_{P_i}^k \Bigg[\delta_i^k \gamma_i^k \chi_{ij}^k \lambda_{ij}^k - \sigma_i^k \left(\beta_{ji}^k \psi_j^k + \sum_n \beta_{ni}^k \lambda_{nj}^k \left(\gamma_n^k - 1 \right) \chi_{nj} \right) \Bigg]. \tag{A45}$$

The matrix for migration dynamics is given by

$$C_{ii}^{kl} = \alpha_{C_i}^k \left[\eta_i^{lk} \omega_i^{lk} - \eta_i^{kl} \hat{\omega}_i^{kl} \right] \tag{A46}$$

and

$$C_{ij}^{kl} = \alpha_{C_i}^k \left[\eta_i^{lk} \kappa_{ij}^{lk} - \eta_i^{kl} \hat{\kappa}_{ij}^{kl} \right]. \tag{A47}$$

6. Niche model topologies

The food webs in Figs. 2 and 3 were generated with the niche model [51]. In this model, each species i is assigned at random a niche value $n_i \in [0,1]$, which is related to the biomass turnover rate α_i occurring in the generalized modeling approach.

Each species is assigned a feeding range r_i and a feeding center c_i. The feeding range is drawn from a β distribution

$$r_i = \left[1 - (1-x)^{\frac{2C}{1-2C}} \right] \cdot n_i \tag{A48}$$

with a random number $x \in [0,1]$, and with C being the connectivity of the food web (see corresponding figure sections for values).

The feeding center c_i is chosen at random from the interval $[\frac{r}{2}, n - \frac{r}{2}]$, and a species $j \neq i$ is a prey of species i if its niche value n_j is within the interval $[c_i - r_i/2, c_i + r_i/2]$. Every species without a prey species is considered a primary producer.

Each prey species is assigned a relative contribution to the diet of its predator, which is drawn from a normal distribution. We subsequently normalize the relative contributions such that they add up to 1.

7. Parametrization of the model

In the following, we assume that all patches are identical and thus $P_{ij}^k = P_{ij}^l$ for all k and l in N. In addition, for simplicity, we assume that the same generalized parameters, which are not based on diet composition or body mass, have identical values for all species, e.g., $\phi_i^k = \phi_j^k \equiv \phi$. Generalized parameters based on diet composition, e.g., β_i^k, are determined by the generated food web. In addition, we assume that biomass flows scale with niche value n_i, which is a proxy for body size [29], i.e., $\alpha_{P_i}^k = 10^{-2n_i}$ and $\alpha_{C_i}^k = 10^{-4n_i}$. The remaining free parameter for the local food webs are ϕ, γ, λ, ψ, and μ. The migration parameters contained in $\mathbf{C}$ are ω, $\tilde{\omega}$, κ, and $\tilde{\kappa}$.

8. Details for Fig. 3

For Fig. 3, we generated niche webs with four species and a connectivity C of 0.33 ± 0.01 until we obtained one with the desired structure shown in Fig. 1, with the niche values shown in Table II. Matrix $\mathbf{P}$ is given by Eqs. (A44) and (A45). The parameters in $\mathbf{P}$ are $\phi = 0.5$, $\gamma = 0.95$, $\lambda = 1$, $\psi = 1.5$, and $\mu = 1.0$.

We assume that the local patch food webs are linked by diffusive migration and therefore $\mathbf{C}$ is given by

$$\mathbf{C} = \begin{pmatrix} 10^{-4 \cdot n_1} & 0 & 0 & 0 \\ 0 & 10^{-4 \cdot n_2} & 0 & 0 \\ 0 & 0 & 10^{-4 \cdot n_3} & 0 \\ 0 & 0 & 0 & 10^{-4 \cdot n_4} \end{pmatrix}. \tag{A49}$$

The entries in $\mathbf{C}$ scale with the inverse niche values and thus inverse body mass, and therefore larger species migrate slower than smaller species. This occurs for instance when small species can be dispersed passively by wind or water, while larger species require energy-consuming active dispersal, are more territorial, or overcome physical barriers less easily.

TABLE II. Niche values, feeding ranges, and centers used for the local food web in Fig. 2 rounded to the second decimal.

i	1	2	3	4
n_i	0.97	0.34	0.91	0.12
c_i	0.42	0.17	0.43	0.06
r_i	0.74	0.34	0.49	0.11

The weighted Laplacian $\mathbf{L}$ for the first spatial geometry used in Figs. 3(a) and 3(d) is given by

$$\mathbf{L} = c \cdot \begin{pmatrix} 2 & -1 & -1 & 0 & 0 \\ -1 & 4 & -1 & -1 & -1 \\ -1 & -1 & 3 & -1 & 0 \\ 0 & -1 & -1 & 2 & 0 \\ 0 & -1 & 0 & 0 & 1 \end{pmatrix} \tag{A50}$$

and the weighted Laplacians used in Figs. 3(b) and 3(c) are given by

$$\mathbf{L} = c \cdot \begin{pmatrix} 1 & 0 & -1 & 0 & 0 \\ 0 & 1 & 0 & -1 & 0 \\ -1 & 0 & 3 & -1 & -1 \\ 0 & -1 & -1 & 3 & -1 \\ 0 & 0 & -1 & -1 & 2 \end{pmatrix}. \tag{A51}$$

For Figs. 3(a) and 3(b), the global coupling strength c is set to 0.045, while it has a value of 0.09 for Fig. 3(c), which results in twice as large eigenvalues κ.

The eigenvalues λ_κ of the full Jacobian are related to the eigenvalues κ of $\mathbf{L}$ by the equation

$$(\mathbf{P} - \kappa \mathbf{C}) \cdot \boldsymbol{q} = \lambda_\kappa \boldsymbol{q}. \tag{A52}$$

The MSF is obtained by solving this equation for all $\kappa \in [0, \kappa_{\max}]$ and plotting the real part of the leading eigenvalue $\mathrm{Re}[\lambda_{\max}(\kappa)]$. In order to obtain the stability of a meta-food web for a given spatial topology, only the eigenvalues κ of the respective Laplacian $\mathbf{L}$ are relevant.

9. Details for Fig. 4

For Fig. 4, we generated a 20-species food web, with a connectivity C of 0.15 ± 0.01. The matrix P for the food web was constructed using the parameters $\phi = 0.5$, $\gamma = 0.75$, $\lambda = 1$, $\psi = 1.0$, and $\mu = 1.0$.

The global coupling strength between the patches is set to 0.045 for Fig. 4(a) and to 0.09 for Fig. 4(b). In addition to diffusive migration, the coupling matrix $\mathbf{C}$ contains cross diffusion which describes adaptive migration, that is, predators follow prey and prey species avoid their predator. Thus, for a predator-prey pair (ij), the submatrix $\mathbf{C_{ij}}$ takes the form

$$\mathbf{C_{ij}} = \begin{pmatrix} 10^{-4 \cdot n_i} & a \cdot 10^{-4 \cdot n_i} \\ -a \cdot 10^{-4 \cdot n_j} & 10^{-4 \cdot n_j} \end{pmatrix} \tag{A53}$$

with $a = 17.22$ for Fig. 4(a) and $a = 0.178$ for Fig. 4(b). All other nondiagonal entries in $\mathbf{C}$ are zero. The parameters used to create the 20-species food webs can be found in Tables III and IV.

10. Details for Fig. 5

The spatial topologies were generated as random geometric graphs [57]. The range R is scaled with the number of nodes N of the spatial graph

$$R = \frac{r}{\sqrt{N}}, \tag{A54}$$

where the parameter r is the unscaled range. For the random geometric graph with $N = 25$ used in Figs. 5(a) and 5(c) the parameter was set to $r = 1.3$. The spatial graph with $N = 500$ used in Figs. 5(b) and 5(d) was generated with $r = 1.4$. Only connected graphs were selected.

For Figs. 5(a) and 5(c), we used a manually constructed five-species food web with the niche values shown in Table V and a connectivity of $C = 0.25$. The feeding links are defined by the weighted adjacency matrix of the local food web

$$\mathbf{A} = \begin{pmatrix} 0 & 0 & 0 & 0 & 0 \\ 0 & 0 & 0 & 0 & 0 \\ 1 & 0 & 0 & 0 & 0 \\ \frac{1}{2} & \frac{1}{2} & 0 & 0 & 0 \\ 0 & 0 & \frac{1}{2} & \frac{1}{2} & 0 \end{pmatrix}. \tag{A55}$$

Species 1 and 2 are primary producers. Predators prey equally on the corresponding prey species. The resulting food web is shown in Fig. 6(a).

TABLE III. Niche values, feeding ranges, and centers for the food web used in Fig. 3(a).

i	1	2	3	4	5	6	7
n_i	0.02	0.69	0.12	0.20	0.54	0.81	0.58
r_i	0.00	0.51	0.02	0.18	0.00	0.18	0.03
c_i	0.010	0.275	0.060	0.100	0.490	0.650	0.115
i	8	9	10	11	12	13	14
n_i	0.65	0.56	0.54	0.51	0.74	0.81	0.80
r_i	0.23	0.03	0.03	0.02	0.17	0.09	0.26
c_i	0.525	0.245	0.235	0.420	0.555	0.495	0.340
i	15	16	17	18	19	20	
n_i	0.88	0.46	0.10	0.19	0.83	0.31	
r_i	0.53	0.12	0.02	0.06	0.25	0.02	
c_i	0.595	0.260	0.080	0.110	0.615	0.150	

TABLE IV. Niche values, feeding ranges, and centers for the food web used in Fig. 3(b).

i	1	2	3	4	5	6	7
n_i	0.41	0.97	0.55	0.95	0.46	0.55	0.85
r_i	0.23	0.49	0.22	0.75	0.20	0.27	0.01
c_i	0.245	0.345	0.480	0.485	0.120	0.265	0.595
i	8	9	10	11	12	13	14
n_i	0.74	0.98	0.03	0.66	0.01	0.05	0.93
r_i	0.16	0.18	0.02	0.06	0.00	0.02	0.43
c_i	0.600	0.74	0.01	0.320	0.010	0.040	0.595
i	15	16	17	18	19	20	
n_i	0.53	0.38	0.49	0.70	0.76	0.93	
r_i	0.41	0.03	0.30	0.07	0.12	0.24	
c_i	0.305	0.035	0.260	0.455	0.550	0.120	

TABLE V. Niche values used for the local food web in Figs. 4(a) and 4(c).

i	1	2	3	4	5
n_i	0.2	0.3	0.4	0.4	0.7

The population dynamics equations used for the explicit simulations are

$$\begin{aligned}\dot{X}_i^k &= G_i^k(X_i^k) - M_i^k(X_i^k) \\ &\quad + F_i^k(X_1^k,\ldots,X_S^k) - \sum_j \frac{R_{ji}^k(X_i^k)F_j^k(T_j^k,X_j^k)}{T_j^k(X_1^k,\ldots,X_S^k)} \\ &\quad + \sum_l \left[E_i^{kl}(X_1^k,\ldots,X_S^k,X_1^l,\ldots,X_S^l)\right. \\ &\quad \left. - E_i^{lk}(X_1^l,\ldots,X_S^l,X_1^k,\ldots,X_S^k)\right], \end{aligned} \tag{A56}$$

with the functions

$$G_i^k(X_i^k) = s_i X_i^k, \tag{A57}$$

$$M_i^k(X_i^k) = p_i X_i^k + q_i {X_i^k}^2, \tag{A58}$$

$$\begin{aligned} F_i^k(X_i^k,\ldots,X_S^k) &= \frac{\sum_j a_i A_{ij} X_i^k X_j^k}{1+\sum_j a_i h_i A_{ij} X_j^k} \\ &= F_i^k(T_i^k,X_i^k) \\ &= \frac{a_i T_i^k X_i^k}{1+a_i h_i T_i^k}, \end{aligned} \tag{A59}$$

$$R_{ij}^k = A_{ij} X_j^k, \tag{A60}$$

$$T_i^k(X_1^k,\ldots,X_S^k) = \sum_j A_{ij} X_j^k, \tag{A61}$$

$$E_i^{kl}(X_i^l) = c_i^{kl} X_i^l. \tag{A62}$$

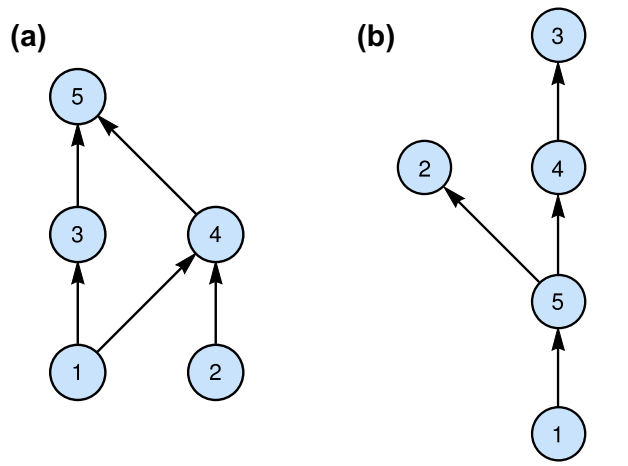

FIG. 6. Five-species food web, used in Figs. 4(a) and 4(c) (a) and for the animated oscillations (b). The shown numbers are the indices of the species. The arrows indicate the direction of biomass flow. In food web (a), species 1 and 2 are the primary producers and species 5 is the apex predator. In network (b) species 1 is the primary producer and species 3 is the observed top predator.

TABLE VI. Parameters for the explicit model in Eqs. (A57)–(A62), and the values used when calculating explicit population dynamics. The parameter s_i is nonzero only for primary producers.

Parameter	Meaning	Value
a_i	Attack rate of Pred.	$4m_i^{-0.25}$
h_i	Handling time of Pred.	$0.26m_i^{-0.25}$
p_i	Linear Mort. Coeff.	$0.52m_i^{-0.25}$
q_i	Quadratic Mort. Coeff.	$0.34m_i^{-0.25}$
c_i	Diffusion Coeff.	$10^{-3}\ m_i^{0.75}$
s_i	Primary Prod. Coeff.	$4.5m_i^{-0.25}$

The predation $F_i^k(X_i^k)$ is based upon the Holling type II functional response. Migration $E_i^{kl}(X_i^k)$ and primary production $G_i^k(X_i^k)$ are in linear proportion to the population sizes while respiration and mortality M_i^k are between linear and quadratic. R_{ij}^k is the relative contribution of species j to the prey consumed by i. T_i^k is the total amount of food available to species i. The adjacency matrix A_{ij} contains the information about the feeding links. The migration term E_i^{kl} scales linearly with population size, i.e., migration is diffusive. The used parameters are shown in Table VI, and the body mass was calculated as

$$m_i = 10^{3n_i}. \tag{A63}$$

If a real leading eigenvalue changes its sign from negative to positive, the system undergoes a Turing instability (Fig. 5). If the leading eigenvalue is complex, a wave instability occurs, which leads to (at least transient) spatiotemporal oscillations. An animation of such an oscillating system is available at http://eco.fkp.physik.tu-darmstadt.de/drossel/gramlich/animation.gif.

In order to investigate the dynamics after an instability occurred, trajectories starting close to the unstable homogeneous state were simulated until they approached a new long term behavior. For these simulations, initial values were chosen randomly with a maximum relative distance of 0.1% to the homogeneous steady state.

11. Details for the animation

The animation shows a comparison of the respective eigenvector (open circles) and the observed deviation from the

TABLE VII. Parameters used for the local food web in the animation.

i	1	2	3	4	5
n_i	0.042	0.865	0.990	0.614	0.257
α_{Pi}	0.824	0.019	0.010	0.0592	0.306
δ_i	0	1	1	1	1
σ_i	0.512	0.000	0.000	0.495	0.668
i,j	2,5	3,4	4,5	5,1	else
β_{ij}	0.457	1.000	0.543	1.000	0.000
A_{ij}	1	1	1	1	0

homogeneous value in the final state (dots). In the right panel, the population density of the top predator [index 3, Fig. 6(b)] is shown. The homogeneous steady state is located at a biomass of 1, larger biomasses are shown in orange and smaller values in blue.

The food web of the oscillating system [Fig. 6(b)] was generated with the niche model. The explicit model was matched to the parameters $\phi = 0.5$, $\gamma = 0.75$, $\psi = 1.5$, and $\mu = 1.0$. Species dependent parameters can be found in Table VII, and the diffusion coefficient is given by

$$c_i = 10 \times 10^{-8n_i}. \tag{A64}$$

The population dynamics is given by

$$\dot{x}_i^k = \alpha_{P_i^k}\Big[\tilde{\delta}_i^k g_i^k\left(x_i^k\right) + \delta_i^k f_i^k\left(t_i^k, x_i^k\right) - \tilde{\sigma}_i^k m_i^k\left(x_i^k\right) - \sigma_i^k \sum_j \beta_{ji}^k d_{ji}^k\left(x_1^k, \ldots, x_S^k\right)\Big] - \sum_l L^{kl} c_i x_i^l, \tag{A65}$$

with

$$g_i^k\left(X_i^k\right) = \left(x_i^k\right)^\phi, \tag{A66}$$

$$m_i^k\left(X_i^k\right) = \left(x_i^k\right)^\mu, \tag{A67}$$

$$f_i^k\left(X_i^k, \ldots, x_S^k\right) = t_i^k\left(x_i^k\right)^\psi \frac{1+K}{t_i^k + K}, \tag{A68}$$

$$d_{ij}^k = \left(x_i^k\right)^\psi x_j^k \frac{1+K}{t_i^k + K}, \tag{A69}$$

$$t_i^k\left(x_1^k, \ldots, x_S^k\right) = \sum_j A_{ij} x_j^k, \tag{A70}$$

where

$$K = \frac{\gamma}{1-\gamma}. \tag{A71}$$

[1] M. E. W. Newman, D. J. Watts, and L. Barabasi, *The Structure and Dynamics of Networks* (Princeton University Press, Princeton, 2006).

[2] A. M. Turing, The chemical basis of morphogenesis, Philos. Trans. R. Soc. London **237**, 37 (1952).

[3] A. Gierer and H. Meinhardt, A theory of biological pattern formation, Kybernetik **12**, 30 (1972).

[4] H. Nakao and A. S. Mikhailov, Turing patterns in network-organized activator-inhibitor systems, Nat. Phys. **6**, 544 (2010).

[5] L. D. Fernandes and M. A. M. de Aguiar, Turing patterns and apparent competition in predator-prey food webs on networks, Phys. Rev. E **86**, 056203 (2012).

[6] L. M. Pecora and T. L. Carroll, Master Stability Functions for Synchronized Coupled Systems, Phys. Rev. Lett. **80**, 2109 (1998).

[7] A. Arenas, A. Díaz-Guilera, J. Kurths, Y. Moreno, and C. Zhou, Synchronization in complex networks, Phys. Rep. **469**, 93 (2008).

[8] A. Pikovsky, J. Kurths, and M. Rosenblum, *Synchronization* (Cambridge University Press, Cambridge, 2001).

[9] R. Parshani, S. V. Buldyrev, and S. Havlin, Interdependent Networks: Reducing the Coupling Strength Leads to a Change from a First to Second Order Percolation Transition, Phys. Rev. Lett. **105**, 048701 (2010).

[10] S. V. Buldyrev, R. Parshani, G. Paul, H. E. Stanley, and S. Havlin, Catastrophic cascade of failures in interdependent networks, Nature (London) **464**, 1025 (2010).

[11] A. Bashan, Y. Berezin, S. V. Buldyrev, and S. Havlin, The extreme vulnerability of interdependent spatially embedded networks, Nat. Phys. **9**, 667 (2013).

[12] M. De Domenico, A. Sole-Ribalta, E. Omodei, S. Gomez, and A. Arenas, Ranking in interconnected multilayer networks reveals versatile nodes, Nat. Commun. **6**, 6868 (2015).

[13] J. Gao, S. V. Buldyrev, H. E. Stanley, and S. Havlin, Networks formed from interdependent networks, Nat. Phys. **8**, 40 (2011).

[14] M. Kivelä, A. Arenas, M. Barthelemy, J. P. Gleeson, Y. Moreno, and M. A. Porter, Multilayer networks, J. Complex Networks **2**, 203 (2014).

[15] M. De Domenico, A. Solé-Ribalta, E. Cozzo, M. Kivelä, Y. Moreno, M. A. Porter, S. Gómez, and A. Arenas, Mathematical Formulation of Multilayer Networks, Phys. Rev. X **3**, 041022 (2013).

[16] S. Boccaletti, G. Bianconi, R. Criado, C. I. del Genio, J. Gómez-Gardeñes, M. Romance, I. Sendiña-Nadal, Z. Wang, and M. Zanin, The structure and dynamics of multilayer networks, Phys. Rep. **544**, 1 (2014).

[17] E. Cozzo, G. F. de Arruda, F. A. Rodrigues, and Y. Moreno, in *Interconnected Networks*, edited by F. Schweitzer and A. Garas (Springer, Heidelberg, 2015).

[18] M. De Domenico, C. Granell, M. A. Porter, and A. Arenas, The physics of spreading processes in multilayer networks, Nat. Phys. **12**, 901 (2016).

[19] M. Asllani, D. M. Busiello, T. Carletti, D. Fanelli, and G. Planchon, Turing patterns in multiplex networks, Phys. Rev. E **90**, 042814 (2014).

[20] X. Zhang, S. Boccaletti, S. Guan, and Z. Liu, Explosive Synchronization in Adaptive and Multilayer Networks, Phys. Rev. Lett. **114**, 038701 (2015).

[21] N. E. Kouvaris, S. Hata, and A. D. Guilera, Pattern formation in multiplex networks, Sci. Rep. **5**, 10840 (2015).

[22] C. I. del Genio, J. Gómez-Gardeñes, I. Bonamassa, and S. Boccaletti, Synchronization in networks with multiple interaction layers, Sci. Adv. **2**, e1601679 (2016).

[23] R. Sevilla-Escoboza, I. Sendiña-Nadal, I. Leyva, R. Gutiérrez, J. M. Buldú, and S. Boccaletti, Inter-layer synchronization in multiplex networks of identical layers, Chaos **26**, 065304 (2016).

[24] L. Tang, X. Wu, J. Lü, J.-a. Lu, and R. M. D'Souza, Master stability functions for multiplex networks, arXiv:1611.09110.

[25] I. Leyva, R. Sevilla-Escoboza, I. Sendiña-Nadal, R. Gutiérrez, J. Buldú, and S. Boccaletti, Inter-layer synchronization in non-identical multi-layer networks, Sci. Rep. **7**, 45475 (2017).

[26] G. E. Hutchinson, Homage to Santa Rosalia or why are there so many kinds of animals? Am. Nat. **93**, 145 (1959).

[27] K. S. McCann, The diversity-stability debate, Nature (London) **405**, 228 (2000).

[28] T. Gross, L. Rudolf, S. A. Levin, and U. Dieckmann, Generalized models reveal stabilizing factors in food webs, Science **325**, 747 (2009).
[29] B. Kartascheff, L. Heckmann, B. Drossel, and C. Guill, Why allometric scaling enhances stability in food web models, Theor. Ecol. **3**, 195 (2010).
[30] R. Levins, Some demographic and genetic consequences of environmental heterogeneity for biological control, Bull. Entomol. Soc. Am. **15**, 237 (1969).
[31] J. D. Yeakel, J. W. Moore, P. R. Guimarães, and M. A. M. de Aguiar, Synchronisation and stability in river metapopulation networks, Ecol. Lett. **17**, 273 (2014).
[32] E. Tromeur, L. Rudolf, and T. Gross, Impact of dispersal on the stability of metapopulations, J. Theor. Biol. **392**, 1 (2016).
[33] P. Pillai, M. Loreau, and A. Gonzalez, A patch-dynamic framework for food web metacommunities, Theor. Ecol. **3**, 223 (2010).
[34] P. Pillai, A. Gonzalez, and M. Loreau, Metacommunity theory explains the emergence of food web complexity, Proc. Natl. Acad. Sci. USA **108**, 19293 (2011).
[35] K. Ristl, S. J. Plitzko, and B. Drossel, Complex response of a food-web module to symmetric and asymmetric migration between several patches, J. Theor. Biol. **354**, 54 (2014).
[36] P. Gramlich, S. J. Plitzko, L. Rudolf, B. Drossel, and T. Gross, The influence of dispersal on a predator-prey system with two habitats, J. Theor. Biol. **398**, 150 (2015).
[37] E. Barter and T. Gross, Meta-food-chains as a many-layer epidemic process on networks, Phys. Rev. E **93**, 022303 (2016).
[38] A. Mougi and M. Kondoh, Food-web complexity, meta-community complexity and community stability, Sci. Rep. **6**, 24478 (2016).
[39] S. Pilosof, M. A. Porter, M. Pascual, and S. Kéfi, The multilayer nature of ecological networks, Nat. Ecol. Evolution **1**, 0101 (2015).
[40] D. Gravel, F. Massol, and M. A. Leibold, Stability and complexity in model meta-ecosystems, Nat. Commun. **7**, 12457 (2016).
[41] T. Gross and U. Feudel, Generalized models as a universal approach to the analysis of nonlinear dynamical systems, Phys. Rev. E **73**, 016205 (2006).
[42] M. R. Hirt, W. Jetz, B. C. Rall, and U. Brose, A general scaling law reveals why the largest animals are not the fastest, Nat. Ecol. Evolution **1**, 1116 (2017).
[43] R. Merris, Laplacian graph eigenvectors, Lin. Algebra Applicat. **278**, 221 (1998).
[44] B. Mohar, Y. Alavi, G. Chartrand, and O. R. Oellermann, The Laplacian spectrum of graphs, Graph Theory, Combinatorics, Applicat. **2**, 871 (1991).
[45] R. Agaev and P. Chebotarev, in *Linear Algebra and Its Applications* (Elsevier, Amsterdam, 2005), Vol. 399, pp. 157–168.
[46] M. Baurmann, T. Gross, and U. Feudel, Instabilities in spatially extended predator-prey systems: Spatio-temporal patterns in the neighborhood of Turing-Hopf bifurcations, J. Theor. Biol. **245**, 220 (2007).
[47] J. D. Yeakel, M. M. Pires, L. Rudolf, N. J. Dominy, P. L. Koch, P. R. Guimarães, and T. Gross, Collapse of an ecological network in Ancient Egypt, Proc. Natl. Acad. Sci. USA **111**, 14472 (2014).
[48] S. J. Plitzko, B. Drossel, and C. Guill, Complexity-stability relations in generalized food-web models with realistic parameters, J. Theor. Biol. **306**, 7 (2012).
[49] C. Kuehn, S. Siegmund, and T. Gross, Dynamical analysis of evolution equations in generalized models, IMA J. Appl. Math. **78**, 1051 (2013).
[50] Y. Nievergelt, The concept of elasticity in economics, SIAM Rev. **25**, 261 (1983).
[51] R. J. Williams and N. D. Martinez, Simple rules yield complex foodwebs, Nature (London) **404**, 180 (2000).
[52] J. D. Yeakel, D. Stiefs, M. Novak, and T. Gross, Generalized modeling of ecological population dynamics, Theor. Ecol. **4**, 179 (2011).
[53] A. Stein, K. Gerstner, and H. Kreft, Environmental heterogeneity as a universal driver of species richness across taxa, biomes and spatial scales, Ecol. Lett. **17**, 866 (2014).
[54] M. Cucuringu and M. W. Mahoney, Localization on low-order eigenvectors of data matrices, arXiv:1109.1355.
[55] A. Nyberg, T. Gross, and K. E. Bassler, Mesoscopic structures and the Laplacian spectra of random geometric graphs, J. Complex Networks **3**, 543 (2014).
[56] C. Dettmann, O. Georgiou, and G. Knight, Spectral statistics of random geometric graphs, Europhys. Lett. **118**, 18003 (2017).
[57] J. Dall and M. Christensen, Random geometric graphs, Phys. Rev. E **66**, 016121 (2002).
[58] J. Guckenheimer and P. Holmes, *Nonlinear Oscillations, Dynamical Systems and the Bifurcations of Vector Fields* (Springer, New York, 1983).